

AD-A119 142

NAVAL UNDERWATER SYSTEMS CENTER NEW LONDON CT NEW LO--ETC F/G 12/1
A TWO-PARAMETER CLASS OF BESSEL WEIGHTINGS WITH CONTROLLABLE SI--ETC(U)
JUL 82 A H NUTTALL

UNCLASSIFIED

NUSC-TR-6761

NL

1 of 1
AD A
M 82

END
DATE
FILMED
10-82
DTIC

①

AD A119142

NUSC Technical Report 6761
1 July 1982

**A Two-Parameter Class of Bessel Weightings
With Controllable Sidelobe Behavior for Linear,
Planar-Circular, and Volumetric-Spherical Arrays;
The Ideal Weighting-Pattern Pairs**

Albert H. Nuttall
Surface Ship Sonar Department

DTIC FILE COPY



Naval Underwater Systems Center
Newport, Rhode Island / New London, Connecticut

DTIC
SEP 13 1982
S
E

Approved for public release; distribution unlimited.

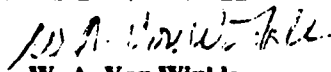
82 09 13 057

Preface

This research was conducted under NUSC Project No. A75205, Subproject No. ZR0000101, "Applications of Statistical Communication Theory to Acoustic Signal Processing," Principal Investigator Dr. Albert H. Nuttall (Code 3302), Program Manager Mr. Robert M. Hillyer, Naval Material Command (MAT 05).

The Technical Reviewer for this report was David T. Porter (Code 3234).

REVIEWED AND APPROVED: 1 July 1982



W. A. Von Winkle
Associate Technical Director for Technology

The author of this report is located at the
Naval Underwater Systems Center, New London Laboratory
New London, Connecticut 06320

REPORT DOCUMENTATION PAGE		READ INSTRUCTIONS BEFORE COMPLETING FORM
1. REPORT NUMBER TR 6761	2. GOVT ACCESSION NO. AD A119142	3. RECIPIENT'S CATALOG NUMBER
4. TITLE (and Subtitle) A TWO-PARAMETER CLASS OF BESSEL WEIGHTINGS WITH CONTROLLABLE SIDELobe BEHAVIOR FOR LINEAR, PLANAR-CIRCULAR, AND VOLUMETRIC-SPHERICAL ARRAYS; THE IDEAL WEIGHTING-PATTERN PAIRS	5. TYPE OF REPORT & PERIOD COVERED	
	5. PERFORMING ORG. REPORT NUMBER	
7. AUTHOR(s) Albert H. Nuttall	6. CONTRACT OR GRANT NUMBER(s)	
9. PERFORMING ORGANIZATION NAME AND ADDRESS Naval Underwater Systems Center New London Laboratory New London, Connecticut 06320	10. PROGRAM ELEMENT, PROJECT, TASK AREA & WORK UNIT NUMBERS A75205 ZR0000101	
11. CONTROLLING OFFICE NAME AND ADDRESS Naval Material Command (MAT O8L) Washington, D.C. 20362	12. REPORT DATE 1 July 1982	
	13. NUMBER OF PAGES 84	
14. MONITORING AGENCY NAME & ADDRESS (if different from Controlling Office)	15. SECURITY CLASS. (of this report) UNCLASSIFIED	
	15a. DECLASSIFICATION/DOWNGRADING SCHEDULE	
16. DISTRIBUTION STATEMENT (of this Report) Approved for public release; distribution unlimited.		
17. DISTRIBUTION STATEMENT (of the abstract entered in Block 20, if different from Report)		
18. SUPPLEMENTARY NOTES		
19. KEY WORDS (Continue on reverse side if necessary and identify by block number)		
Bessel Weightings	Ideal Weighting	Generalized Functions
Windows	Approximations to	Mainlobe Width
Sidelobe Control	Generalized Functions	Null Location
Planar Arrays	Ideal Windows	
Volumetric Arrays	Pattern Characteristics	
20. ABSTRACT (Continue on reverse side if necessary and identify by block number)		
<p>A two-parameter class of Bessel weightings is presented whose patterns have controllable sidelobe decay and mainlobe-to-peak-sidelobe ratio, for one-, two-, and three-dimensional arrays. In the one-dimensional application, the class of weightings subsumes the Kaiser-Bessel weighting as a special case, and extends to the ideal van der Maas weighting as a limiting case. In the two- and three-dimensional applications, all the results are new; the ideal patterns in these latter cases are also derived and found to require weightings with</p>		

1501

20. (Cont'd)

generalized functions that are more singular than the delta functions required for one dimension. Approximations to the generalized functions are presented.

LIST OF ILLUSTRATIONS

<u>Figure</u>	<u>Page</u>
1 Normalized Weighting for $\nu = 2$	11
2 Normalized Weighting for $\nu = 1.5$	11
3 Normalized Weighting for $\nu = 1$	12
4 Normalized Weighting for $\nu = .5$	12
5 Normalized Weighting for $\nu = 0$	13
6 Normalized Weighting for $\nu = -.5$	13
7 Ideal Pattern $g_i(u)$	16
8 Pattern in dB for $\alpha = 2$	18
9 Pattern in dB for $\alpha = 1.5$	19
10 Pattern in dB for $\alpha = 1$	20
11 Pattern in dB for $\alpha = .5$	21
12 Pattern in dB for $\alpha = 0$	22
13 Pattern in dB for $\alpha = -.5$	22
14 First Null Location of Pattern $g(u) = J_\alpha(\sqrt{u^2 - B^2})$	25
15 Peak Sidelobe Level of Pattern $g(u) = J_\alpha(\sqrt{u^2 - B^2})$	28
16 Peak Sidelobe Level Versus First Null Location of Pattern $g(u) = J_\alpha(\sqrt{u^2 - B^2})$	29
A-1 Geometry for Planar Array	37
F-1 Approximation to Auxiliary Function A(s)	62
F-2 Approximation to Generalized Function G(s)	62
F-3 An Alternative Approximation to Generalized Function G(s)	64
F-4 An Approximation to Weighting (50)	64
F-5 Final Approximation to Weighting (50)	67
F-6 Pattern of Approximation (F-12) for $\epsilon = .1$	68
F-7 Pattern of Approximation (F-12) for $\epsilon = .01$	69
F-8 Pattern of Approximation (F-12) for $\epsilon = .001$	70
F-9 Pattern of Approximation (F-14) for $\epsilon = .2$	71
F-10 Pattern of Approximation (F-14) for $\epsilon = .15$	72
F-11 Pattern of Approximation (F-14) for $\epsilon = .1$	73

LIST OF TABLES

	<u>Page</u>
1. Identification of Values of μ in (11)	4
2. First Zero of $J_\alpha(z)$	24
3. Weighting-Pattern Pairs; $\mu > -1$	31
4. Required Weighting for Ideal Pattern	32

LIST OF SYMBOLS

R	radius or half-length of array
λ	wavelength of plane-wave arrival
ϕ_a, θ_a	arrival angles of plane wave
ϕ_l, θ_l	look angles of array
s	normalized distance on array
w(s)	normalized weighting of array
g(u)	voltage response pattern of array
u	dimensionless parameter of array; (4), (6), (8)
$J_\alpha(x)$	Bessel function of order α and argument x
$I_\alpha(x)$	modified Bessel function of order α and argument x
K	kernel of transform (10)
μ	parameter indicating dimensionality of array; table 1
$J_\alpha(z)$	Bessel function ratio, (17)
$Q_\alpha(z)$	Bessel function ratio, (18)
v, B	weighting parameters, (22)
$\Gamma(x)$	gamma function
α	composite order of Bessel function, (29)
$g_i(u)$	ideal pattern, (34)
z_α	smallest nonzero null location of $J_\alpha(z)$, (38)
u_0	first null location of pattern g(u)
u_p	first sidelobe peak location of g(u)
sub G	generalized function, (50)

A TWO-PARAMETER CLASS OF BESSEL WEIGHTINGS WITH CONTROLLABLE
SIDELOBE BEHAVIOR FOR LINEAR, PLANAR-CIRCULAR, AND VOLUMETRIC-
SPHERICAL ARRAYS; THE IDEAL WEIGHTING-PATTERN PAIRS

INTRODUCTION

A wide variety of time-domain weightings for spectral analysis, whose frequency-domain windows have very good sidelobe behavior, have been presented in [1,2]. Since the basic mathematics describing the response of a weighted linear array can also be written as a Fourier transform, these weighting-window pairs have immediate application to one-dimensional array processing as well as spectral analysis.

Most of the weighting-window pairs in [1,2] have no parameters in their design equations; that is, the windows are fixed and cannot be altered, as for example, in the Hanning and Hamming windows. A few windows, such as the Dolph-Chebyshev and Kaiser-Bessel [3,4], do have a single parameter in their design equations that allows for a tradeoff between the mainlobe width and the ratio of mainlobe to peak sidelobe. However, neither have any control over the rate of decay of the sidelobes, the Dolph-Chebyshev case having no decay, and the Kaiser-Bessel case a 6 dB/octave decay. It is obvious that in order to control both the sidelobe decay and the mainlobe-to-peak-sidelobe ratio, a two-parameter family of weightings is necessary. And it is desirable (although not necessary) for the window to possess a simple analytical form that can be easily understood and evaluated for a range of parameter values. Such a class of Bessel weightings is presented in this report.

For the array application, the weighting is applied as a multiplicative factor in the spatial domain; the response to plane wave arrivals from various directions is called the pattern, rather than the window. Here we will give a two-parameter family of weighting-pattern pairs for use with arrays in one, two, or three dimensions, and shall indicate the ideal weightings and corresponding patterns in all cases. Special cases of this family will be shown to include some of the weightings that are currently employed in array and signal processing.

RESPONSES OF ONE-, TWO-, AND THREE-DIMENSIONAL ARRAYS

LINEAR ARRAY

We consider a continuous line array located on the x-axis in the range $(-R, R)$ and subject to symmetric weighting $w_1(x)$ for $|x| \leq R$. For a single-frequency plane wave of wavelength λ , arriving at angle θ_a relative to the normal to the line array, the array voltage response, by use of time-delay steering to look-angle θ_l , is

$$g(u) = \int_{-R}^R dx \exp \left[-i2\pi \frac{x}{\lambda} (\sin \theta_a - \sin \theta_l) \right] w_1(x). \quad (1)$$

By letting $s = x/R$ and by using the symmetry of weighting w_1 , we can express response (1) as

$$g(u) = \int_0^1 ds \left(\frac{2}{\pi} \right)^{1/2} \cos(us) w(s), \quad (2)$$

where normalized weighting

$$w(s) = (2\pi)^{1/2} R w_1(Rs), \quad (3)$$

and dimensionless parameter

$$u = 2\pi \frac{R}{\lambda} (\sin \theta_a - \sin \theta_l) \quad (4)$$

incorporates the relevant features of array geometry, look angle, and the arrival wavelength and angle.

Thus the response (2) of a line array is a cosine transform of the normalized weighting. As an example, rectangular weighting yields response $g(u)$ proportional to $\sin u/u$, which has its first few nulls at $u = \pi, 2\pi, 3\pi$.

PLANAR ARRAY

The voltage response of a continuous planar-circular array of radius R , to a plane wave of wavelength λ arriving at (polar, azimuthal) angles (θ_a, ϕ_a) , and subject to weighting which depends only on the distance from the center of the array, is derived in appendix A, culminating in the result (A-11). It is

$$g(u) = \int_0^1 ds s J_0(us) w(s), \quad (5)$$

where $w(s)$ is the normalized weighting and

$$u = 2\pi \frac{R}{\lambda} \left[\sin^2 \theta_\ell + \sin^2 \theta_a - 2 \sin \theta_\ell \sin \theta_a \cos(\phi_\ell - \phi_a) \right]^{1/2}. \quad (6)$$

Here (θ_ℓ, ϕ_ℓ) are the (polar, azimuthal) look angles; that is, the response (5) of a planar-circular array is a zero-th order Bessel transform of the normalized weighting. As an example, rectangular weighting w yields response $g(u)$ proportional to $J_1(u)/u$, which has its first few nulls at $u = 3.83, 7.02, 10.17$.

VOLUMETRIC ARRAY

The voltage response of a continuous volumetric-spherical array of radius R , with weighting dependent only on the distance from the center of the array, is derived in appendix B. The result is given by (B-10) in the form

$$g(u) = \int_0^1 ds \left(\frac{2}{\pi}\right)^{1/2} s \frac{\sin(us)}{u} w(s), \quad (7)$$

where now

$$u = 2\pi \frac{R}{\lambda} \left[2 - 2 \cos \theta_\ell \cos \theta_a - 2 \sin \theta_\ell \sin \theta_a \cos(\phi_\ell - \phi_a) \right]^{1/2}. \quad (8)$$

The other parameters are as explained in the previous subsection.

Equation (7) has the basic form of a sine transform. As an example, rectangular weighting w yields response $g(u)$ proportional to

$$\frac{\sin u - u \cos u}{u^3}, \quad (9)$$

which has its first few nulls at $u = 4.49, 7.73, 10.90$.

UNIFIED FORM FOR ARRAY RESPONSES IN DIFFERENT DIMENSIONS

The results in (2), (5), and (7) for the array voltage response in one, two, and three dimensions, respectively, appear to be quite different. However, they can all be written in the basic form

$$g(u) = \int_0^1 ds K(u, s) w(s), \quad (10)$$

where the kernel

$$K(u, s) = s \left(\frac{s}{u}\right)^\mu J_\mu(us) = \left. \begin{cases} \left(\frac{2}{\pi}\right)^{1/2} \cos(us) & \text{for } \mu = -\frac{1}{2} \\ s J_0(us) & \text{for } \mu = 0 \\ \left(\frac{2}{\pi}\right)^{1/2} s \frac{\sin(us)}{u} & \text{for } \mu = \frac{1}{2} \end{cases} \right\}. \quad (11)$$

Here J_μ is a Bessel function of order μ , and we have used [5; 10.1.1, 10.1.11, 10.1.12]. Thus all the responses are basically Bessel transforms of the normalized weighting w , with the correspondences given in the following table.

Table 1. Identification of Values of μ in (11)

<u>Number of Dimensions</u>	<u>Value of μ</u>
1	-1/2
2	0
3	1/2

If we substitute (11) in (10), we have the explicit result for the response pattern:

$$g(u) = \int_0^1 ds s \left(\frac{s}{u}\right)^\mu J_\mu(us) w(s). \quad (12)$$

Inspection of the properties of the Bessel function reveals that $g(u)$ as given by (12) is even in u ; see [5; 9.1.10]. Thus we only need to investigate $g(u)$ for $u \geq 0$.

HANKEL TRANSFORM PAIRS

The Hankel transform pair of order μ is given by [6; page 136]

$$\begin{aligned} f(u) &= \int_0^{\infty} ds (us)^{\frac{1}{2}} J_{\mu}(us) F(s) \text{ for } u > 0, \\ F(s) &= \int_0^{\infty} ds (su)^{\frac{1}{2}} J_{\mu}(su) f(u) \text{ for } s > 0. \end{aligned} \quad (13)$$

Thus knowledge of either function f or F for positive arguments enables determination of the other function by an integral transform. Under the identification

$$F(s) = s^{\mu+\frac{1}{2}} w(s), \quad f(u) = u^{\mu+\frac{1}{2}} g(u), \quad (14)$$

(13) takes the form

$$g(u) = \int_0^{\infty} ds s \left(\frac{s}{u}\right)^{\mu} J_{\mu}(us) w(s) \text{ for } u > 0, \quad (15)$$

$$w(s) = \int_0^{\infty} du u \left(\frac{u}{s}\right)^{\mu} J_{\mu}(su) g(u) \text{ for } s > 0. \quad (16)$$

Equation (15) is more general than (12) in that it allows for weighting $w(s)$ to be nonzero for $s > 1$. Equation (16) is complementary in that, given a desired pattern $g(u)$, it indicates what weighting $w(s)$ is required for $s > 0$. However, if we attempt to specify some desirable pattern $g(u)$, and then solve (16) for the required weighting $w(s)$, it will generally turn out that the resultant $w(s)$ will be nonzero for $s > 1$. Thus not any pattern $g(u)$ can be selected if we insist on a finite-support weighting $w(s)$; rather, desirable candidate patterns can be substituted in (16) and the corresponding weighting $w(s)$ evaluated to see if it is zero for $s > 1$. If not, the candidate pattern is disallowed and must be modified or discarded.* We will use precisely this procedure in a later section when we determine the weightings that realize the ideal patterns in various numbers of dimensions.

* If pattern $g(u)$ yields $w(s) = 0$ for $s > a$, the scaled pattern $g(u/a)$ yields a modified weighting $a^{2\mu+2} w(as)$, which is zero for $s > 1$, as desired.

DEFINITION OF TWO BESSEL FUNCTION RATIOS

It will be very convenient notationally in the following to employ the shorthand notations

$$J_{\alpha}(z) \equiv \frac{J_{\alpha}(z)}{z^{\alpha}} = \frac{1}{2^{\alpha}} \sum_{k=0}^{\infty} \frac{(-z^2/4)^k}{k! \Gamma(\alpha+1+k)}, \quad (17)$$

$$Q_{\alpha}(z) \equiv \frac{I_{\alpha}(z)}{z^{\alpha}} = \frac{1}{2^{\alpha}} \sum_{k=0}^{\infty} \frac{(z^2/4)^k}{k! \Gamma(\alpha+1+k)}, \quad (18)$$

for these two Bessel function ratios; these types of functions have already been encountered in (11), (12), (15), (16). They are extensions of the $\Psi_n(z)$ functions discussed in [7; page 56]. Both functions, $J_{\alpha}(z)$ and $Q_{\alpha}(z)$, are single-valued and are entire in z for any α , as well as being entire in α for any z [5; 6.1.3, 9.1.1]. Special cases of these functions that are useful here are given by [5; 9.6.6, 10.1.1, 10.1.11, 10.1.12, 10.2.13, 10.2.14]

$$\begin{aligned} Q_{\alpha}(0) &= J_{\alpha}(0) = \frac{1}{2^{\alpha} \Gamma(\alpha+1)}, \\ Q_0(z) &= I_0(z), \quad Q_1(z) = \frac{I_1(z)}{z}, \quad Q_{-1}(z) = z I_1(z), \\ Q_{1/2}(z) &= \left(\frac{2}{\pi}\right)^{1/2} \frac{\sinh z}{z}, \quad Q_{-1/2}(z) = \left(\frac{2}{\pi}\right)^{1/2} \cosh z, \\ Q_{3/2}(z) &= \left(\frac{2}{\pi}\right)^{1/2} \frac{z \cosh z - \sinh z}{z^3}, \quad Q_{3/2}(z) = \left(\frac{2}{\pi}\right)^{1/2} (z \sinh z - \cosh z), \\ Q_{5/2}(z) &= \left(\frac{2}{\pi}\right)^{1/2} \frac{(3+z^2) \sinh z - 3z \cosh z}{z^5}, \\ Q_{-5/2}(z) &= \left(\frac{2}{\pi}\right)^{1/2} [(3+z^2) \cosh z - 3z \sinh z]. \end{aligned} \quad (19)$$

A useful property, which is obvious from (17) and (18) and which will find frequent application here, is

$$J_{\alpha}(\pm iz) = \mathcal{U}_{\alpha}(z), \quad \mathcal{U}_{\alpha}(\pm iz) = J_{\alpha}(z). \quad (20)$$

These relations hold true for all values of z , real or complex. Properties similar to (19) can be obtained for the $J_{\alpha}(z)$ functions; for example,

$$J_{-1/2}(z) = \mathcal{U}_{-1/2}(\pm iz) = \left(\frac{2}{\pi}\right)^{1/2} \cosh(\pm iz) = \left(\frac{2}{\pi}\right)^{1/2} \cos(z).$$

Other useful properties follow from the use of [5; 9.1.30 and 9.6.28],

$$J_{\alpha}'(z) = -z J_{\alpha+1}(z), \quad \mathcal{U}_{\alpha}'(z) = z \mathcal{U}_{\alpha+1}(z), \quad (21)$$

and from [5; 9.1.27 and 9.6.26],

$$\mathcal{U}_{\alpha}(z) = \frac{1}{z^2} \left[\mathcal{U}_{\alpha-2}(z) - 2(\alpha-1) \mathcal{U}_{\alpha-1}(z) \right],$$

$$J_{\alpha}(z) = -\frac{1}{z^2} \left[J_{\alpha-2}(z) - 2(\alpha-1) J_{\alpha-1}(z) \right].$$

A CLASS OF BESSEL WEIGHTINGS

The class of Bessel weightings that we are suggesting, regardless of the number of dimensions of the array, is given by

$$w(s) = \left(\frac{\sqrt{1-s^2}}{B}\right)^{\nu} I_{\nu}\left(B\sqrt{1-s^2}\right) \text{ for } 0 < s < 1, \quad \text{where } \nu > -1, B > 0, \quad (22)$$

and $w(s) = 0$ for $s > 1$. There are two real parameters in this class, namely, ν and B . For the special case of $\nu = 0$, this weighting is already known as Kaiser-Bessel [3,4]; its pattern has nearly the optimum energy content within a specified bandwidth in the one-dimensional application to spectral analysis.

Substitution of (22) in (12) or (15) yields the closed form for the pattern [6; page 30, fourth integral, and 5; 9.6.3]

$$g(u) = \int_0^1 ds s\left(\frac{s}{u}\right)^{\mu} J_{\mu}(us) \left(\frac{\sqrt{1-s^2}}{B}\right)^{\nu} I_{\nu}\left(B\sqrt{1-s^2}\right) \quad (23A)$$

$$= J_{\mu+\nu+1}\left(\sqrt{u^2-B^2}\right) = J_{\mu+\nu+1}\left(\sqrt{B^2-u^2}\right) \text{ for all } u, \text{ if } \mu > -1 \text{ and } \nu > -1. \quad (23B)$$

Here we have employed definitions (17) and (18) and used (20). The condition on μ guarantees convergence of integral (12) at $s = 0$, whereas the condition on ν guarantees convergence of integral (12) at $s = 1$. The first form of (23B) is more convenient computationally for $u \geq B$, whereas the second form is more convenient for $B \geq u$.

Weighting-pattern pair (22)-(23) are the fundamental results for the class of Bessel weightings under consideration. They apply to one-, two-, or three-dimensional arrays when μ is specialized to $-\frac{1}{2}$, 0, or $\frac{1}{2}$, respectively, and when u is interpreted as (4), (6), or (8), respectively. The parameter B is nonnegative and will be shown to control the ratio of mainlobe to peak sidelobe. For the case of one dimension, $\mu = -\frac{1}{2}$, the kernel of transform (23A) is a cosine (see the top line of (11)); in this special case,

the pattern $J_{\nu+\frac{1}{2}}\left(\sqrt{u^2-B^2}\right)$ was also independently and simultaneously discovered by Roy Streit [8].

WEIGHTING CHARACTERISTICS

Weighting (22) is positive for $0 \leq s < 1$ since $\nu > -1$ and $B \geq 0$; see [5; 9.6.10]. In addition, it is zero and therefore continuous at $s = 1$ if $\nu > 0$. In fact [5; 9.6.7],

$$w(s) \sim \frac{(1-s)^\nu}{\Gamma(\nu+1)} \quad \text{as } s \rightarrow 1-. \quad (24)$$

For $\nu \geq 0$, weighting $w(s)$ is monotonically decreasing in s on $(0,1)$; see appendix C. However, for $-1 < \nu < 0$, $w(s)$ possesses an integrable singularity at $s = 1$.

Examples of weighting (22) are plotted in figures 1-6 for $\nu = 2, 1.5, 1, .5, 0, -.5$, respectively. Figure 5, for $\nu = 0$, corresponds to the Kaiser-Bessel weighting [3]. For the larger values of ν , the weighting blends smoothly to zero at $s = 1$, but for the smaller values of ν , the behavior of $w(s)$ is more irregular at $s = 1$, being discontinuous for $\nu = 0$ and infinite for $\nu < 0$. The larger values of B lead to smoother functions that are Gaussian-like; in fact, for $s < 1$ [5; 9.7.1],

$$w(s) \sim \frac{\exp(B)}{(2\pi B)^{\frac{1}{2}} B^\nu} \exp\left(-\frac{1}{2} B^2 s^2\right) \quad \text{as } B \rightarrow \infty. \quad (25)$$

More generally,

$$w(s) \sim (2\pi)^{-\frac{1}{2}} B^{-2\nu} \left(B\sqrt{1-s^2}\right)^{\nu-\frac{1}{2}} \exp\left(B\sqrt{1-s^2}\right) \quad \text{as } B\sqrt{1-s^2} \rightarrow \infty. \quad (26)$$

The opposite limit for small B is

$$w(s) = \left(\frac{1-s^2}{2}\right)^\nu \quad \text{for } B = 0. \quad (27)$$

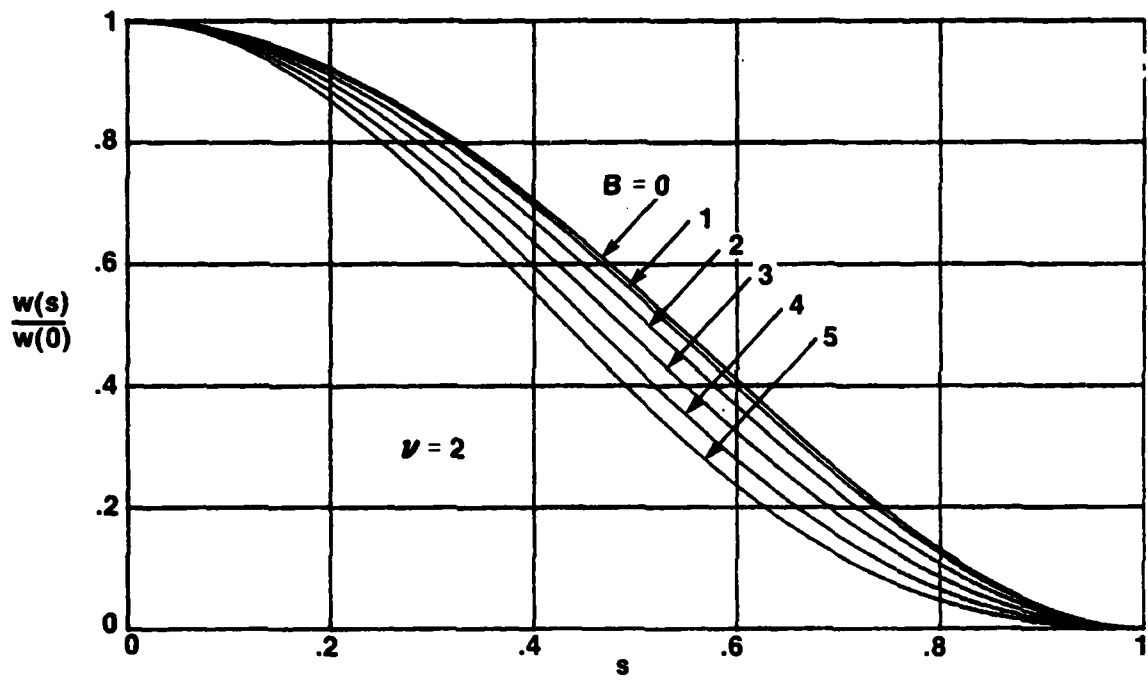


Figure 1. Normalized Weighting for $\nu = 2$

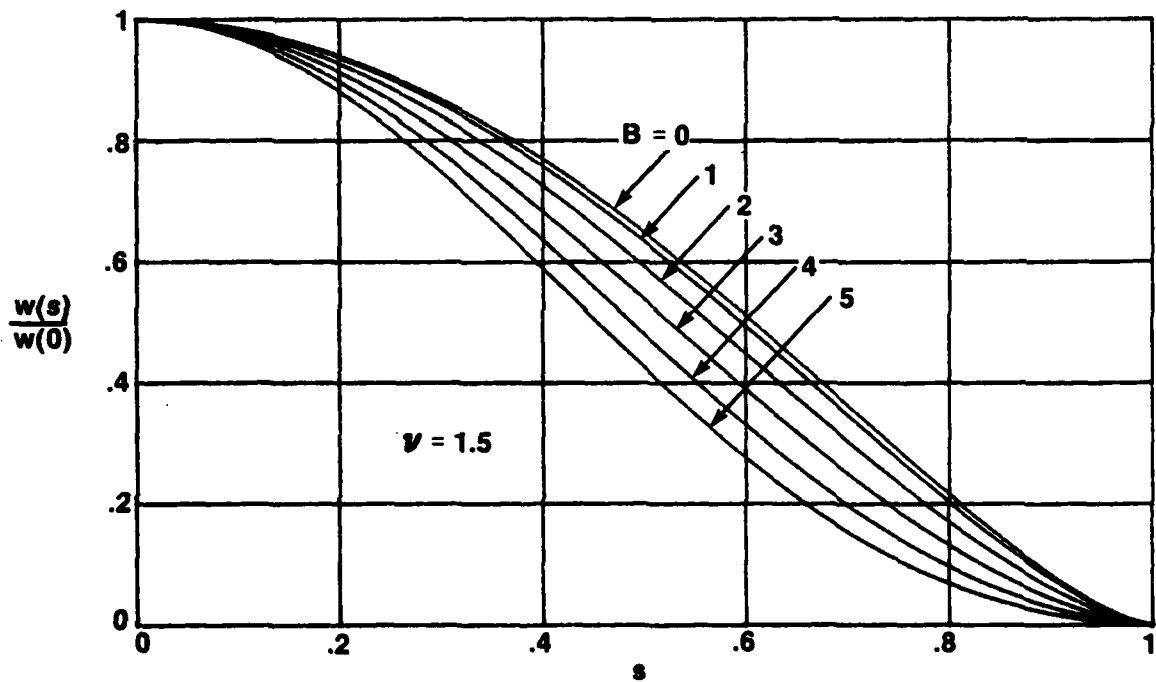


Figure 2. Normalized Weighting for $\nu = 1.5$

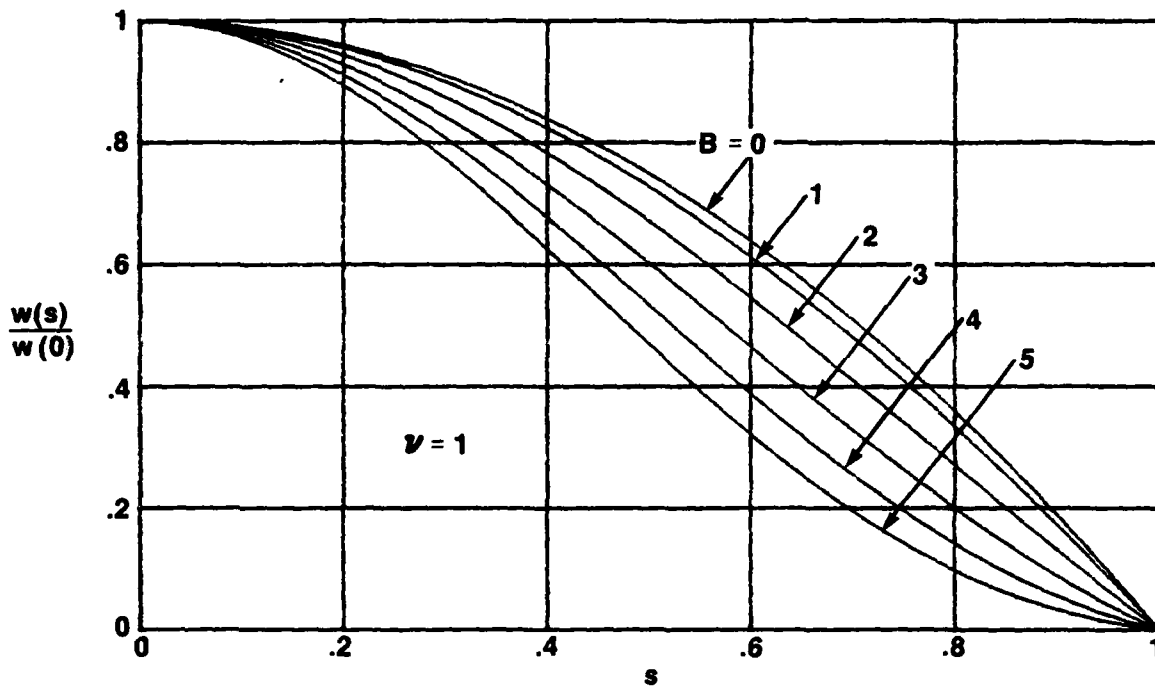


Figure 3. Normalized Weighting for $\nu = 1$

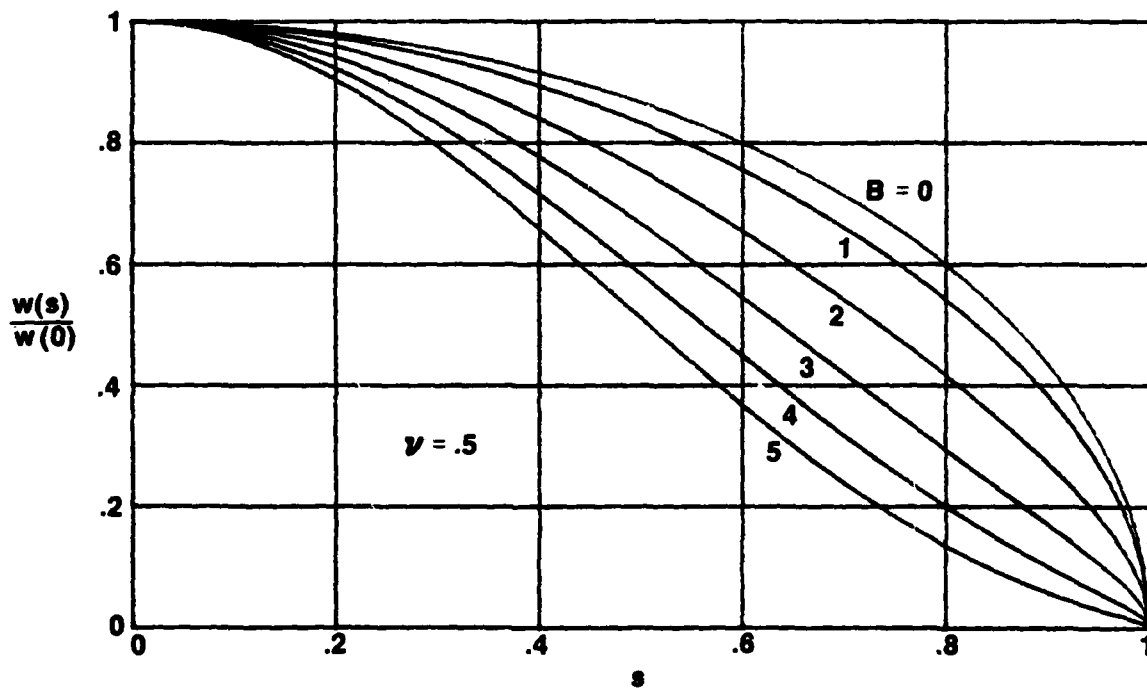


Figure 4. Normalized Weighting for $\nu = .5$

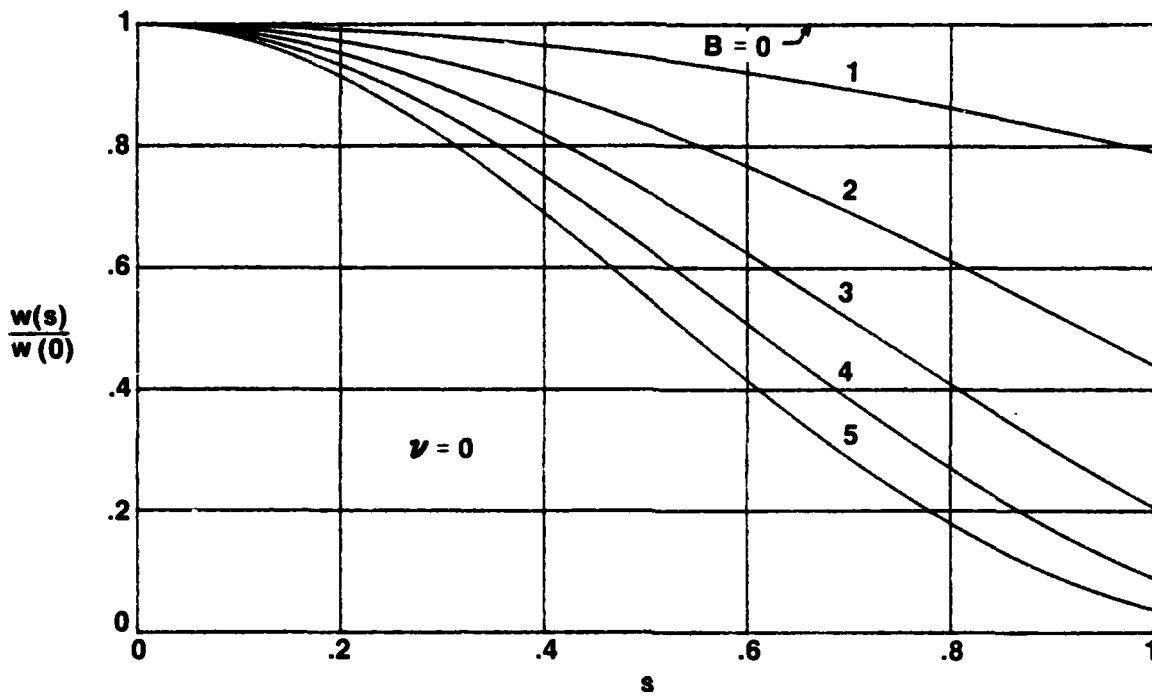


Figure 5. Normalized Weighting for $\nu = 0$

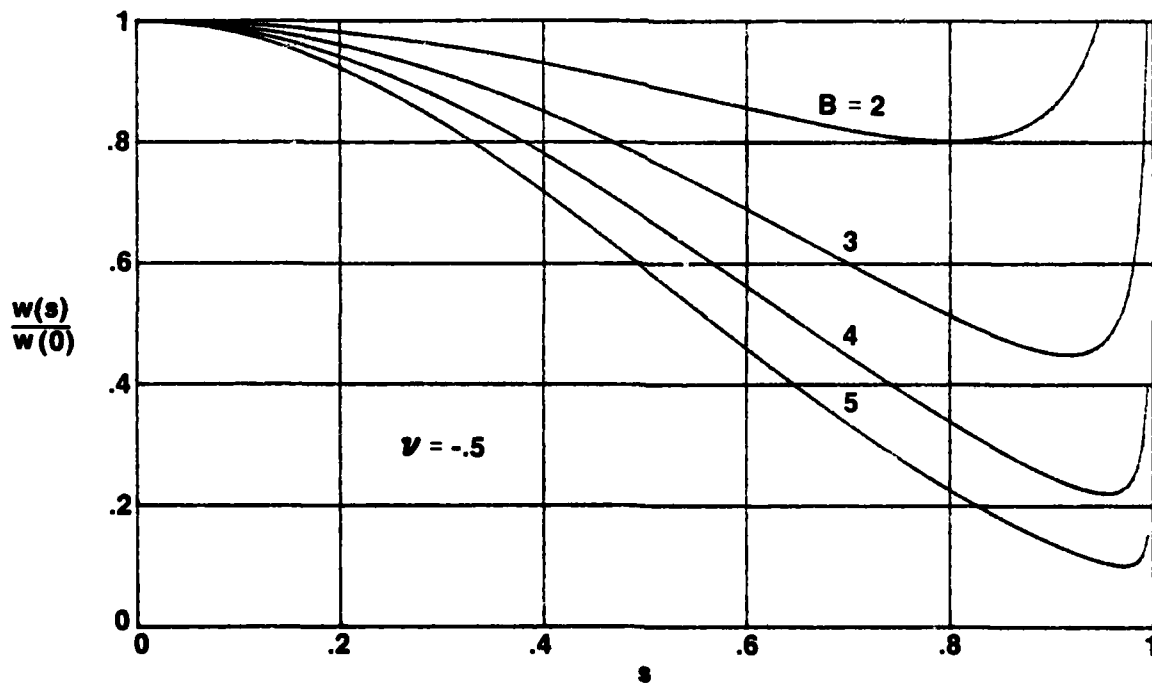


Figure 6. Normalized Weighting for $\nu = -.5$

RESPONSE PATTERN CHARACTERISTICS

The pattern was given by (23) as

$$g(u) = J_{\alpha}(\sqrt{u^2 - B^2}) = J_{\alpha}(\sqrt{B^2 - u^2}), \quad (28)$$

where the composite order of the Bessel function is

$$\alpha = \mu + \nu + 1. \quad (29)$$

The asymptotic behavior of the pattern (28) for large u is available from (17) and [5; 9.2.1]:

$$g(u) \sim \left(\frac{2}{\pi}\right)^{\frac{\nu}{2}} \frac{\cos\left(u - \frac{1}{2}\alpha\pi - \frac{1}{4}\pi\right)}{u^{\alpha + \frac{1}{2}}} \text{ as } u \rightarrow \infty. \quad (30)$$

Since g is proportional to the array voltage response, (30) corresponds to a

$$\text{decay} \sim 6\alpha + 3 \text{ dB/octave as } u \rightarrow \infty. \quad (31)$$

Expressed in terms of the original dimension-parameter μ and weighting-parameter ν , this is, from (29),

$$\begin{aligned} &\text{decay} \sim 6\mu + 6\nu + 9 \text{ dB/octave as } u \rightarrow \infty \\ &= \left. \begin{aligned} &6\nu + 6 \text{ dB/octave for one dimension} \\ &6\nu + 9 \text{ dB/octave for two dimensions} \\ &6\nu + 12 \text{ dB/octave for three dimensions} \end{aligned} \right\}. \quad (32) \end{aligned}$$

Thus the greater the number of dimensions, the faster is the rate of decay of the sidelobes of the response, for a common value of weighting-parameter ν . Each additional dimension adds a 3 dB/octave decay, for a fixed ν .

Special cases of the pattern (28) are available upon use of (19) and (20); for example,

$$g(u) = \left\{ \begin{array}{l} \left(\frac{2}{\pi}\right)^{1/2} \cosh(\sqrt{B^2-u^2}) = \left(\frac{2}{\pi}\right)^{1/2} \cos(\sqrt{u^2-B^2}) \quad \text{for } \alpha = -\frac{1}{2} \\ I_0(\sqrt{B^2-u^2}) = J_0(\sqrt{u^2-B^2}) \quad \text{for } \alpha = 0 \\ \left(\frac{2}{\pi}\right)^{1/2} \frac{\sinh(\sqrt{B^2-u^2})}{\sqrt{B^2-u^2}} = \left(\frac{2}{\pi}\right)^{1/2} \frac{\sin(\sqrt{u^2-B^2})}{\sqrt{u^2-B^2}} \quad \text{for } \alpha = \frac{1}{2} \\ \frac{I_1(\sqrt{B^2-u^2})}{\sqrt{B^2-u^2}} = \frac{J_1(\sqrt{u^2-B^2})}{\sqrt{u^2-B^2}} \quad \text{for } \alpha = 1 \end{array} \right\}. \quad (33)$$

All of these relations are valid for all u , whether u is larger or smaller than B ; of course, the former form in each line is more convenient for $u \leq B$, while the latter is more convenient for $u \geq B$. The third result in (33), for $\alpha = \frac{1}{2}$, includes the pattern in one dimension ($\mu = -\frac{1}{2}$, $\nu = 0$) for the Kaiser-Bessel weighting $I_0(B\sqrt{1-s^2})$ for $0 < s < 1$.

The special case of $\alpha = -\frac{1}{2}$ in (33) deserves extra attention; this case will be called the ideal pattern:

$$\begin{aligned} g_{\frac{1}{2}}(u) &= \mathcal{L}_{-\frac{1}{2}}(\sqrt{B^2-u^2}) = \mathcal{J}_{-\frac{1}{2}}(\sqrt{u^2-B^2}) \\ &= \left(\frac{2}{\pi}\right)^{1/2} \cosh(\sqrt{B^2-u^2}) = \left(\frac{2}{\pi}\right)^{1/2} \cos(\sqrt{u^2-B^2}) \quad \text{for } \alpha = -\frac{1}{2}. \end{aligned} \quad (34)$$

The plot in figure 7 reveals that the sidelobes are all equal, and that the

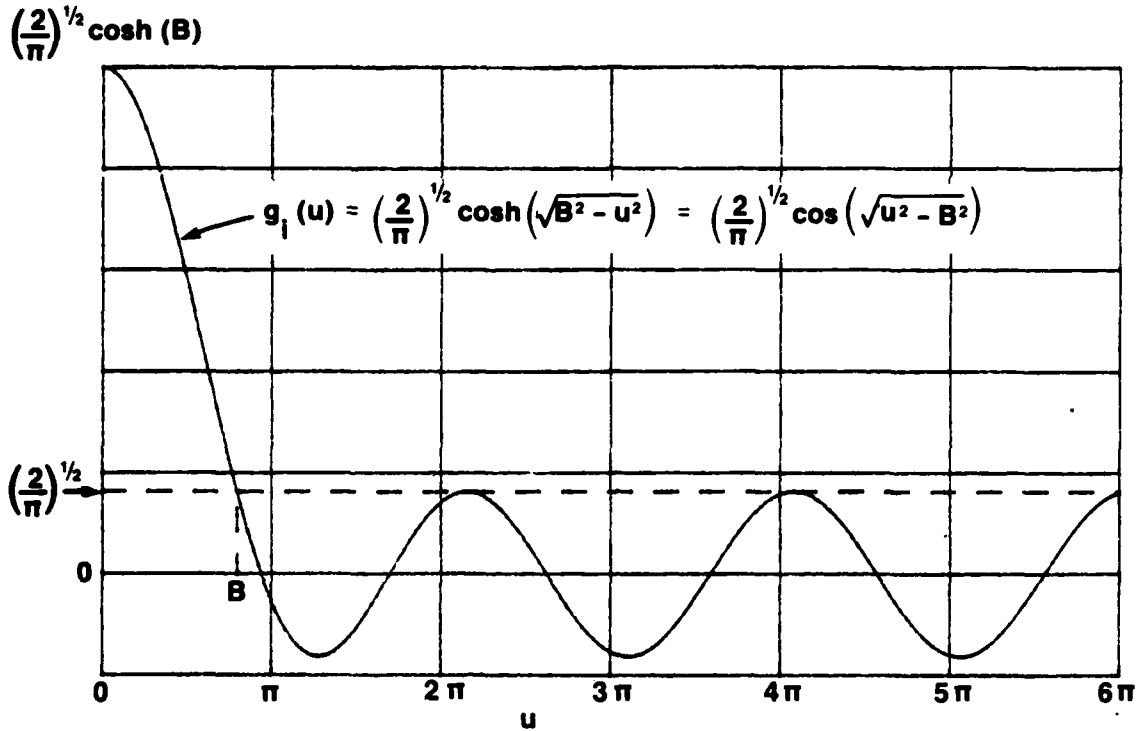


Figure 7. Ideal Pattern $g_i(u)$

voltage ratio

$$\frac{\text{mainlobe level}}{\text{sidelobe level}} = \cosh(B). \quad (35)$$

The mainlobe width, as measured to the point where the mainlobe first decays to the eventual sidelobe level, is

$$\text{mainlobe width} = B. \quad (36)$$

The abscissa u is given by (4), (6), or (8) for one, two, or three dimensions, respectively. Determination of the required weighting to realize the ideal pattern (34) in different numbers of dimensions is taken up in a later section.

If $\alpha < -\frac{1}{2}$, the pattern (28) has increasing sidelobes as u increases; see (30). Therefore, $\alpha \geq -\frac{1}{2}$ are the only cases of practical interest for pattern (28).

Plots of pattern (28) are given in dB in figures 8-13 for $\alpha = 2, 1.5, 1, .5, 0, -.5$, respectively, for various values of B . The program is listed in appendix D. The larger values of α realize the more rapid decay of sidelobes, but, on the other hand, have wider mainlobes. Figures 8-13 indicate the necessary tradeoffs between mainlobe width, sidelobe decay, and mainlobe-to-sidelobe ratio that must be considered in any weighting selection.

A small chart in the upper right quadrant of each figure indicates some allowable values of μ and ν that apply to that figure. For example, in figure 8, the pattern for $\alpha = 2$ applies to all the following:

$$\begin{aligned} \mu &= -\frac{1}{2} \text{ (one dimension) with } \nu = \frac{3}{2}, \\ &\text{or} \\ \mu &= 0 \text{ (two dimensions) with } \nu = 1, \\ &\text{or} \\ \mu &= \frac{1}{2} \text{ (three dimensions) with } \nu = \frac{1}{2}. \end{aligned} \quad (37)$$

When we come to figure 11, for $\alpha = .5$, however, the case of $\mu = \frac{1}{2}$, $\nu = -1$ has an asterisk next to the $\nu = -1$ entry. The reason for this is that the integral (23) leading to pattern $g(u)$ was convergent only for $\nu > -1$, and now we are trying to violate that condition. A similar cautionary note is indicated in figures 12 and 13; in fact, all three cases in figure 13 violate the condition $\nu > -1$. Despite this preclusion, we shall find later that the required weighting does, in fact, have the form (22) for the corresponding ν values given in figures 11 - 13, but requires generalized functions with singularities at the endpoint $s = 1$ of the interval. This extension to $\nu \leq -1$ is desirable and important because realization of the ideal pattern (figures 7 and 13) requires values for ν in this region, regardless of the number of dimensions.

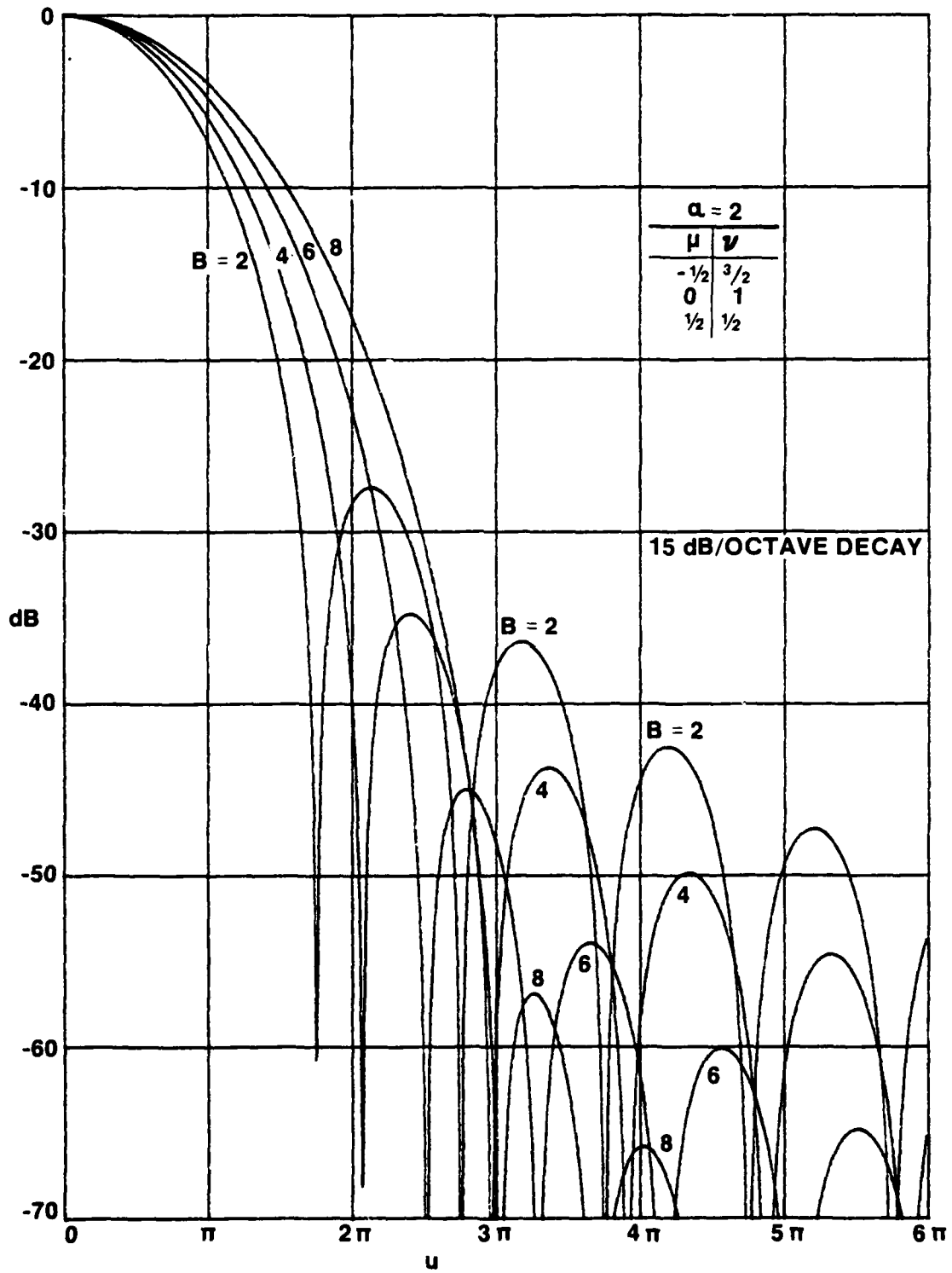


Figure 8. Pattern in dB for $\alpha = 2$

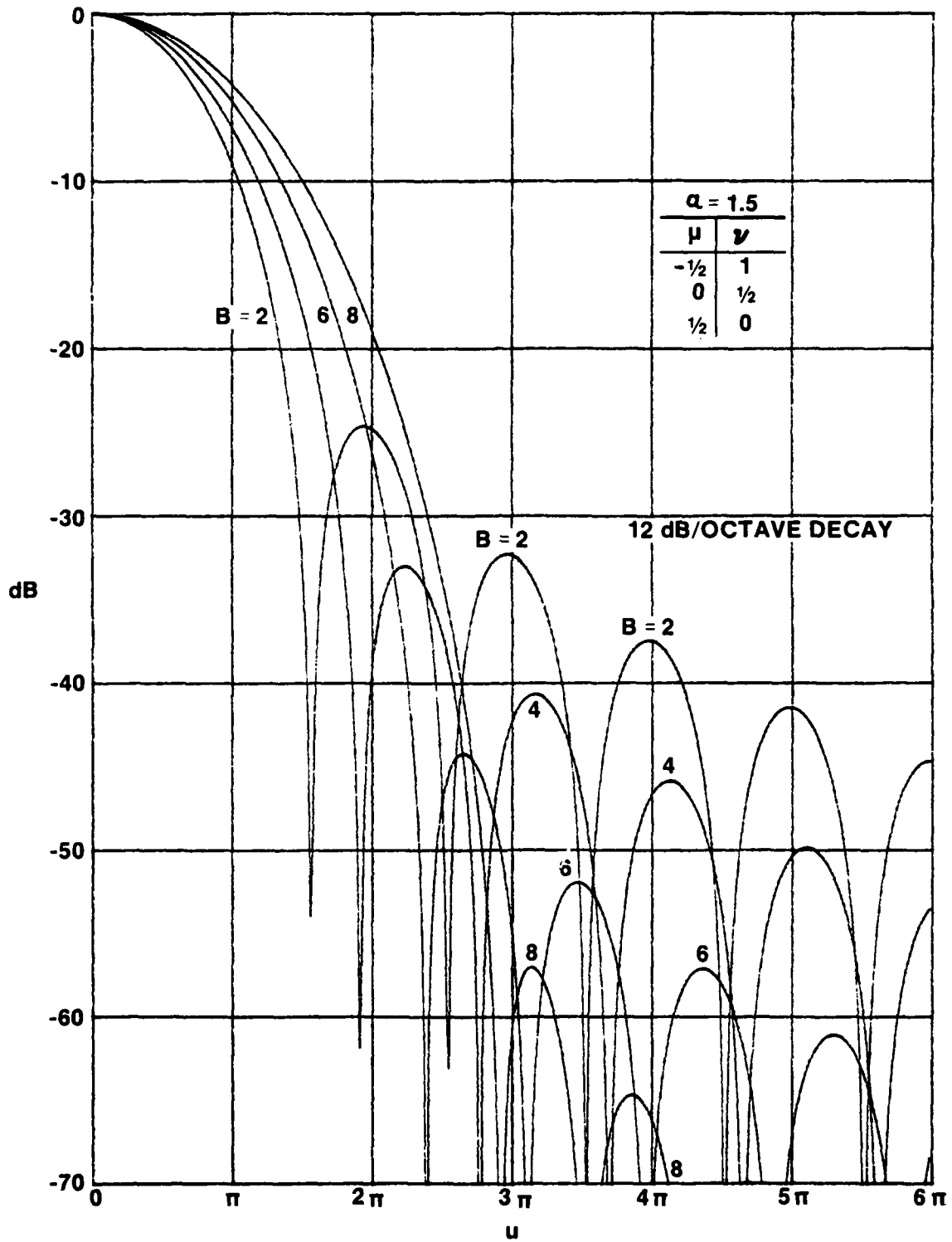


Figure 9. Pattern in dB for $\alpha = 1.5$

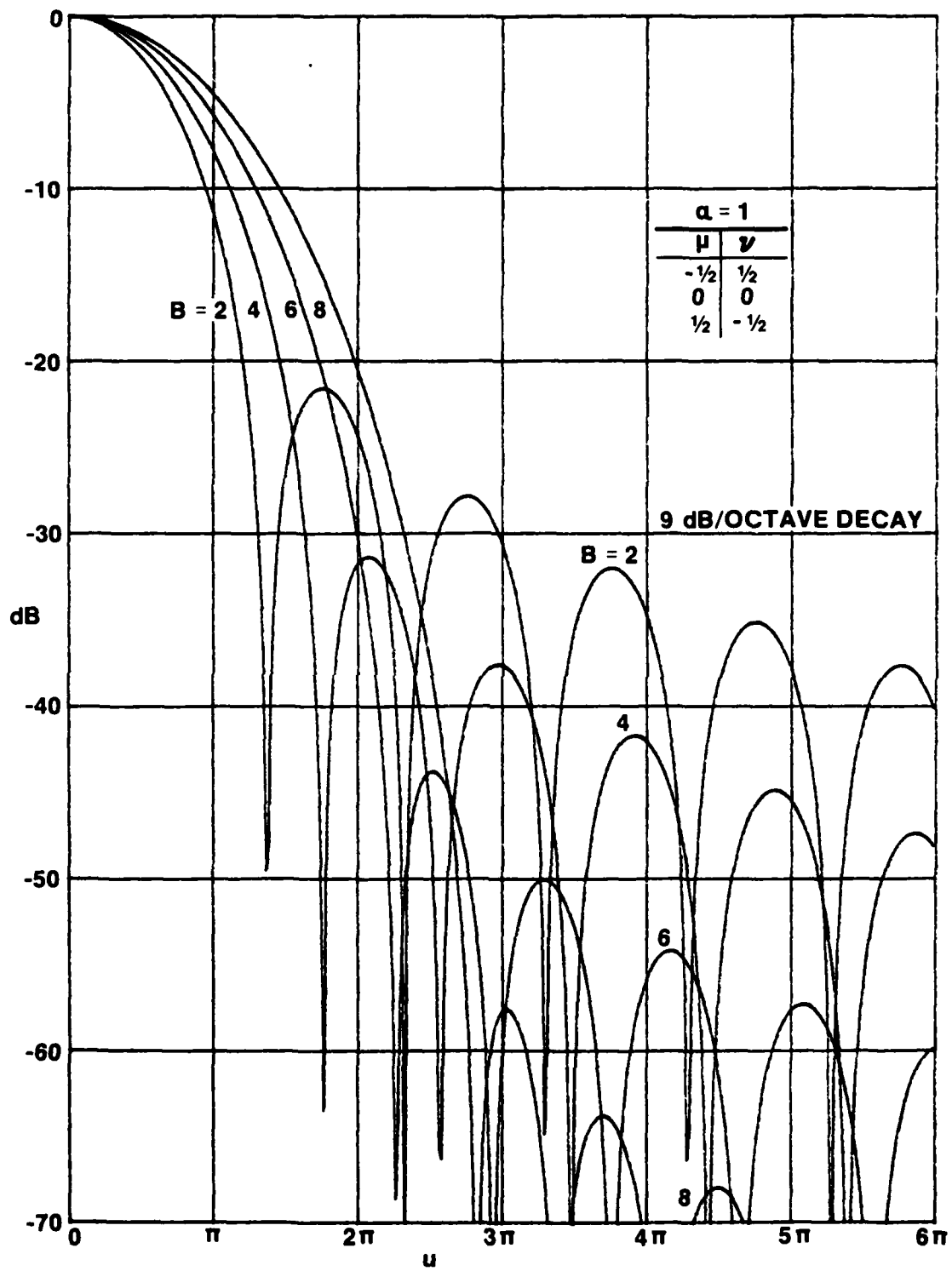


Figure 10. Pattern in dB for $\alpha = 1$

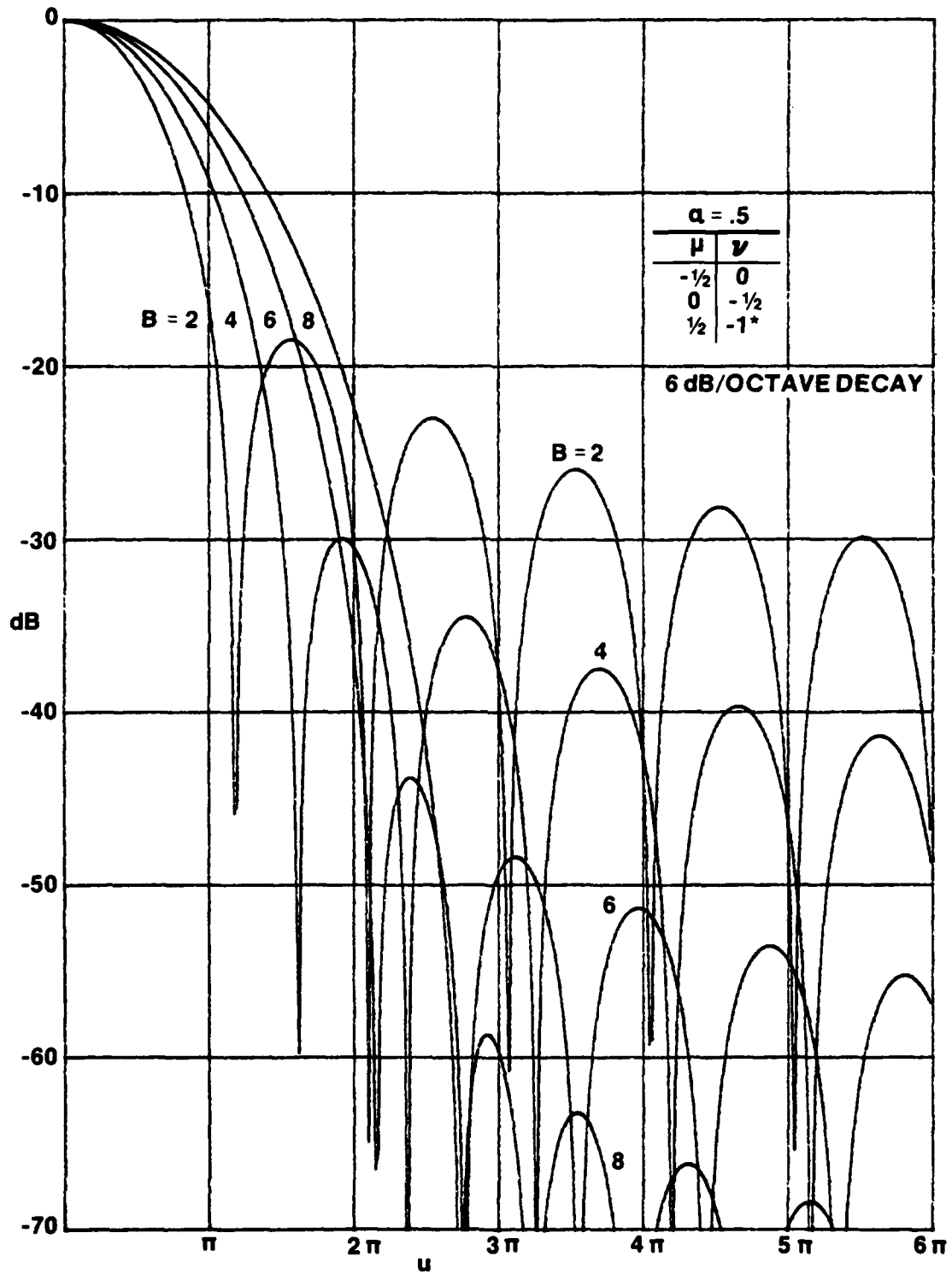


Figure 11. Pattern in dB for $\alpha = .5$

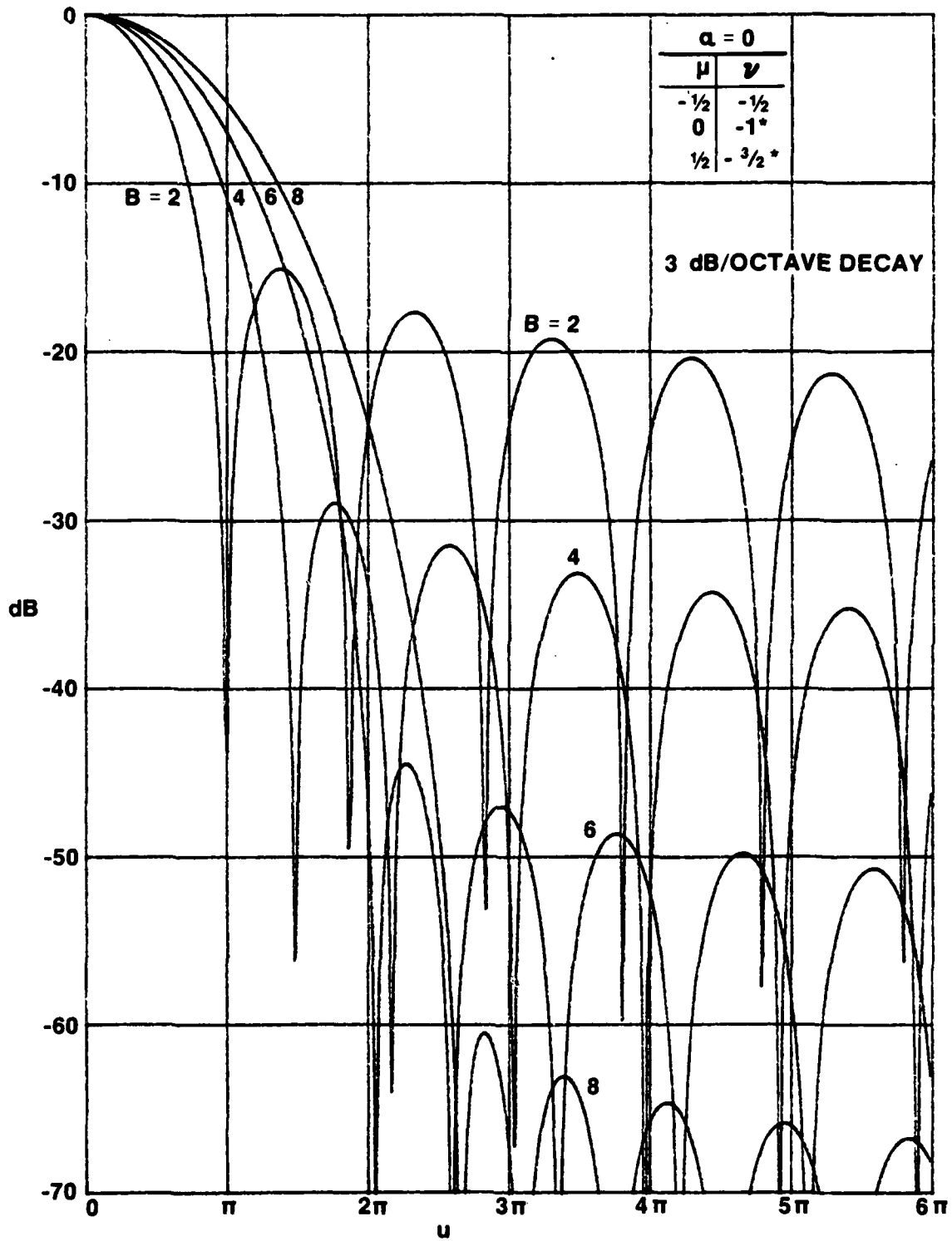


Figure 12. Pattern in dB for $\alpha = 0$

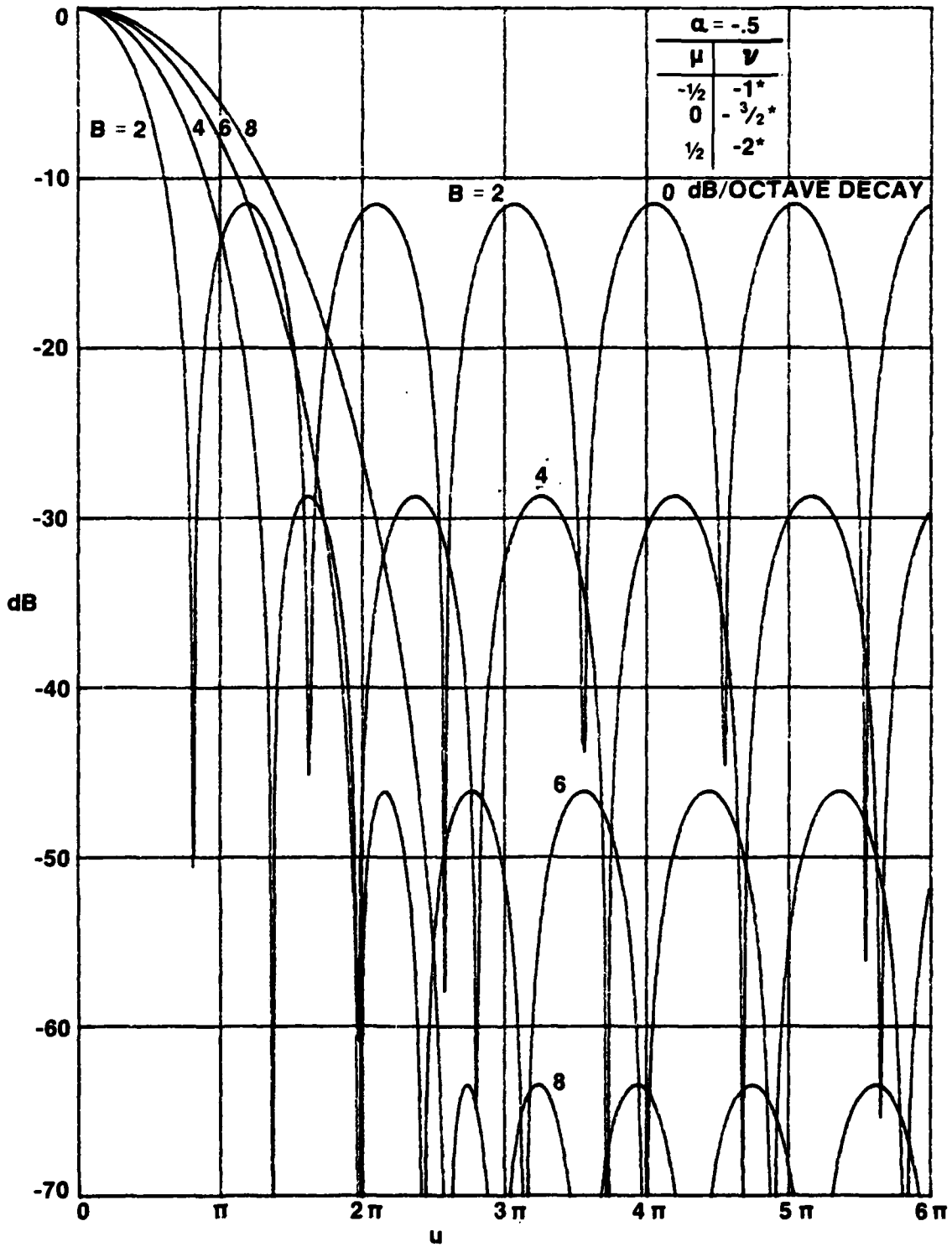


Figure 13. Pattern in dB for $\alpha = -.5$

FIRST NULL LOCATION

Let z_α be the smallest nonzero null location of $J_\alpha(z)$; i.e.,

$$J_\alpha(z_\alpha) = 0. \quad (38)$$

A short list of $\{z_\alpha\}$ is given below in table 2. Then, by use of (17), the

Table 2. First Zero of $J_\alpha(z)$

α	z_α
-0.5	1.5708
0.0	2.4048
0.5	3.1416
1.0	3.8317
1.5	4.4934
2.0	5.1356
2.5	5.7635
3.0	6.3802
3.5	6.9879
4.0	7.5883
4.5	8.1826

first null location of pattern $g(u)$ in (28) is at u_0 , where

$$\left(u_0^2 - B^2\right)^{1/2} = z_\alpha, \quad u_0 = \left(B^2 + z_\alpha^2\right)^{1/2}. \quad (39)$$

The results in figure 14 display the first null location as a function of B , for various values of α . For large B , u_0 behaves as $B + \frac{1}{2}z_\alpha^2/B$. By the identification of α as $\mu + \nu + 1$, this curve applies to any number of dimensions and to whatever value of ν is selected in weighting $w(s)$ of (22). The curves indicate that the first null location u_0 is monotonically increasing in both B and α .

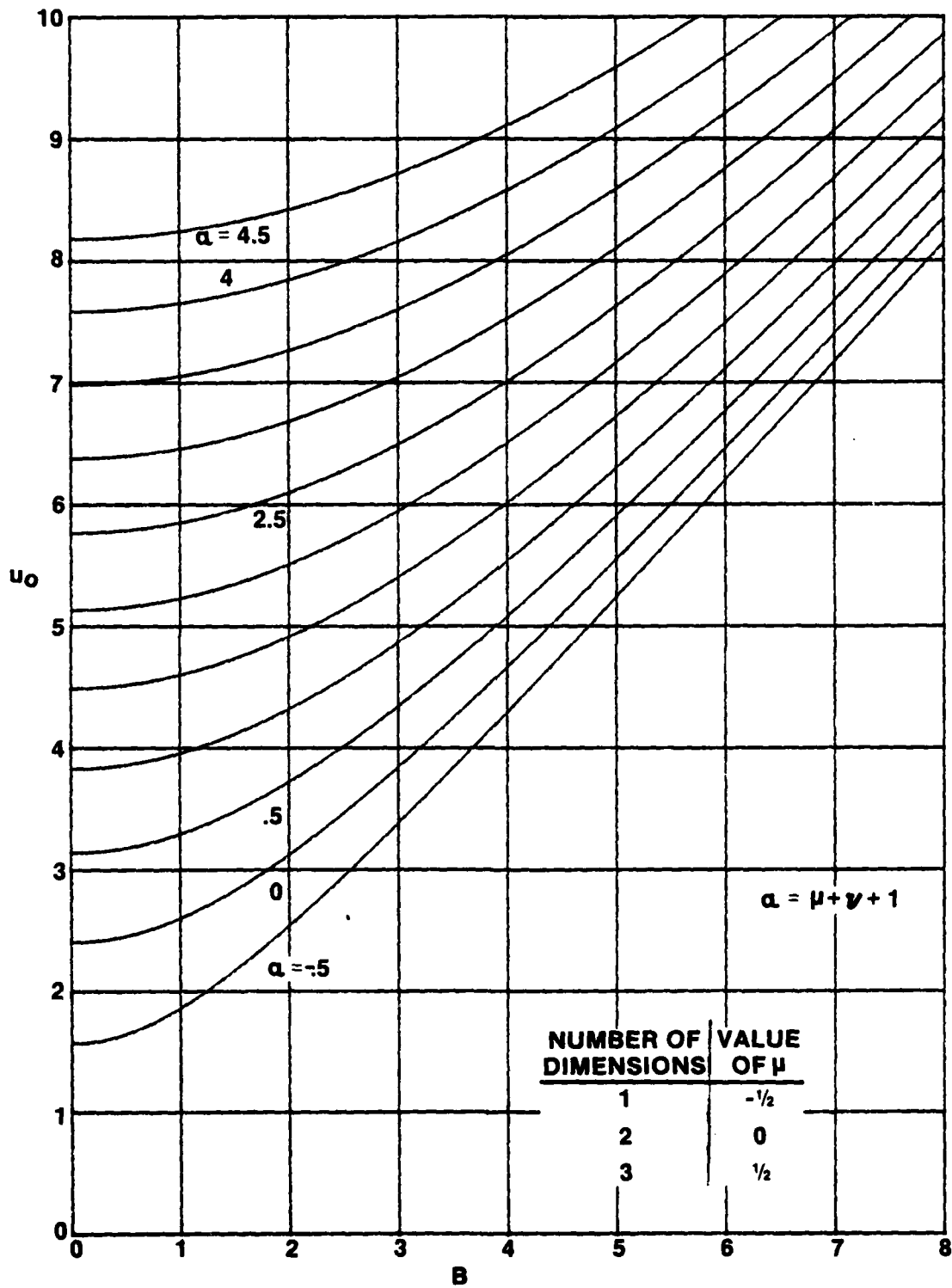


Figure 14. First Null Location of Pattern $g(u) = J_{\alpha}(\sqrt{u^2 - B^2})$.

LOCATION OF PEAK OF FIRST SIDELobe

By use of (28) and (21), we obtain derivative

$$g'(u) = J'_\alpha(\sqrt{u^2 - B^2}) \frac{u}{\sqrt{u^2 - B^2}} = -u J_{\alpha+1}(\sqrt{u^2 - B^2}). \quad (40)$$

Therefore, reference to (38) reveals that the location of the peak of the first sidelobe of $g(u)$ occurs where $g'(u_p) = 0$; i.e.,

$$\left(u_p^2 - B^2\right)^{\frac{1}{2}} = z_{\alpha+1}, \quad u_p = \left(B^2 + z_{\alpha+1}^2\right)^{\frac{1}{2}}. \quad (41)$$

If we employ more explicit notation in (39) and (41), we can express the first peak location in terms of the first null location according to

$$u_p(B, \alpha) = u_0(B, \alpha+1). \quad (42)$$

Thus all the results in figure 14 can be applied directly to the first peak location. For example, (42) yields

$$u_p(B, -\frac{1}{2}) = u_0(B, \frac{1}{2}); \quad (43)$$

thus the third curve from the bottom in figure 14 gives the location of the peak of the first sidelobe when $\alpha = -\frac{1}{2}$.

PEAK SIDELobe LEVEL

The value of voltage pattern $g(u)$ at location (41) gives the level of the peak sidelobe:

$$g(u_p) = J_\alpha(\sqrt{u_p^2 - B^2}) = J_\alpha(z_{\alpha+1}). \quad (44)$$

Since the origin value of the pattern is

$$g(0) = J_{\alpha}(z), \quad (45)$$

the voltage ratio of peak sidelobe level to mainlobe height is

$$\frac{g(u_p)}{g(0)} = \frac{J_{\alpha}(z_{\alpha+1})}{J_{\alpha}(B)}. \quad (46)$$

Relation (46) is plotted in dB in figure 15 as a function of B, for various values of α ; i.e.,

$$\text{dB} = 10 \log \left[\frac{J_{\alpha}(z_{\alpha+1})}{J_{\alpha}(B)} \right]^2. \quad (47)$$

The peak sidelobe level decreases monotonically with increasing B, but has no simple behavior versus α except for very small B or very large B.

The results of these last two figures are combined in figure 16, where we plot the peak sidelobe level in dB versus the first null location u_0 . These latter curves are virtually linear over a wide range. If we disregard the sidelobe decay rate, the most desirable region of this figure is in the lower left quadrant, i.e., small u_0 and very negative dB. However, the closest we can get (from our family) is the $\alpha = -.5$ curve, which is, in fact, the ideal pattern; see (34) and figure 7. Furthermore, the sidelobe decay rate is then 0 dB/octave. Higher sidelobe decay rates are attained by moving toward the upper right quadrant of the figure; for example, the $\alpha = 3.5$ curve has a $6\alpha+3 = 24$ dB/octave sidelobe decay rate. This figure furnishes a very compact display of the important interrelationships that occur between the fundamental features of peak sidelobe level, mainlobe width, and sidelobe decay rate, and allows for a quick tradeoff comparison of alternatives.

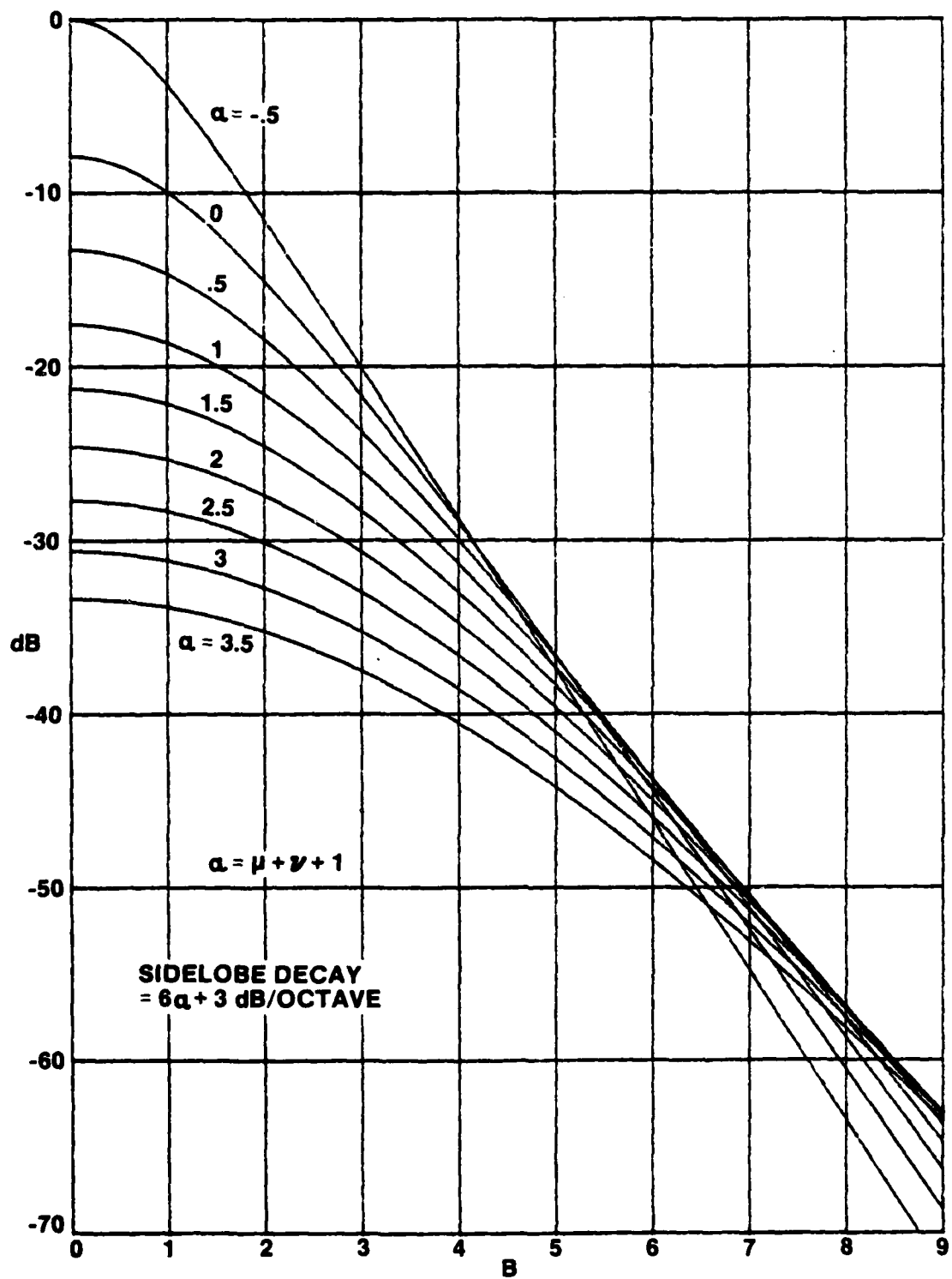


Figure 15. Peak Sidelobe Level of Pattern $g(u) = J_\alpha(\sqrt{u^2 - B^2})$

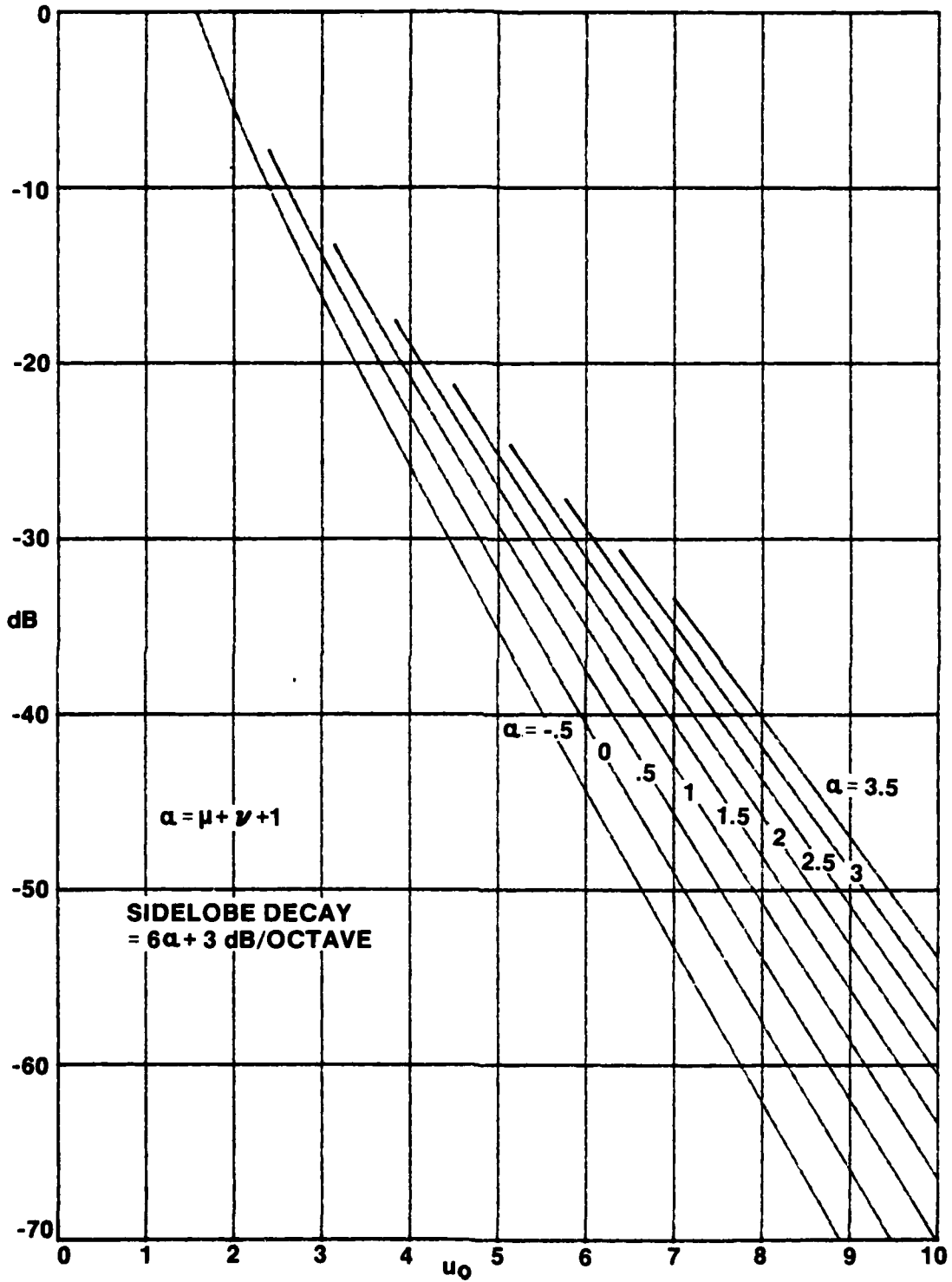


Figure 16. Peak Sidelobe Level Versus First Null Location of Pattern

$$g(u) = J_{\alpha}(\sqrt{u^2 - B^2})$$

IDEAL WEIGHTING AND PATTERN

It was shown in figure 7, in the previous section, that the pattern $g(u)$ for $\alpha = -\frac{1}{2}$ takes on a particularly desirable behavior, namely, a narrow mainlobe width and a large ratio of mainlobe-to-peak-sidelobe. However, figures 11 - 13 indicated that realization of some patterns was apparently not possible in certain dimensions because we were violating the condition on parameter ν in weighting (22) that allowed for convergence of integral (23). Here we will address the more general problem of how to realize pattern (23),

$$g(u) = \int_{u+\nu+1}^{\infty} \sqrt{u^2 - B^2} \quad \text{for all } u, \quad (48)$$

for any $u > -1$, but without the current restriction of $\nu > -1$ in weighting (22). This procedure will of course require a different and more general weighting than (22), and will furnish solutions to the asterisked cases in figures 11 - 13.

The solution for the required weightings to realize (48) for any $u > -1$ is conducted in appendix E. All the weightings are zero for $s > 1$, as desired; their values for $0 \leq s \leq 1$ are listed below. From (E-14),

$$w(s) = \frac{B}{(1-s^2)^{\nu/2}} I_1(B\sqrt{1-s^2}) + \delta(s-1) \quad \text{for } \nu = -1; \quad (49)$$

from (E-33),

$$w(s) = \left(\frac{\sqrt{1-s^2}}{B} \right)^{\nu} I_{\nu}(B\sqrt{1-s^2}) - \frac{(1-s^2)^{\nu}}{2^{\nu}\Gamma(\nu+1)} + \frac{(1-s^2)^{\nu}}{2^{\nu}\Gamma(\nu+1)} \Big|_G \quad \text{for } -2 < \nu < -1; \quad (50)$$

and from (E-39),

$$w(s) = \frac{B^2}{1-s^2} I_2(B\sqrt{1-s^2}) + \left(\frac{B^2}{2} - 1 \right) \delta(s-1) - \delta'(s-1) \quad \text{for } \nu = -2. \quad (51)$$

The extended range for $\nu < -2$ is given in (E-35) and (E-36). Weighting (49) requires a generalized function, namely, a delta function, with its singularity located at $s = 1$. Weighting (51) requires, in addition, the

derivative of a delta function, located at $s = 1$. The intermediate cases in weighting (50) require a generalized function with its singularity located at $s = 1$; interpretation and approximation of this generalized function is given in appendix F.

It can be observed from (49)-(51) that the leading term of $w(s)$ is exactly what would have been obtained from initial weighting (22) by substituting the appropriate value of ν ; here we are using $I_{-\nu}(z) = I_{\nu}(z)$ [5; 9.6.6]. However, the price of crossing the "natural boundary" at $\nu = -1$, which was originally required for (23), is a generalized function with its singularity located at $s = 1$. And the further we go below $\nu = -1$, the more singular becomes the required generalized function; these points are elaborated upon in appendix F.

The explicit assignment of ν values in (48)-(51) leads to table 3 for the weighting-pattern pairs. With regard to application of (48)-(51) to the array

Table 3. Weighting-Pattern Pairs; $\mu > -1$

<u>Weighting</u>	<u>Pattern</u>
(49)	$J_{\mu}(\sqrt{u^2 - B^2})$
(50) with $\nu = -\frac{3}{2}$	$J_{\mu - \frac{1}{2}}(\sqrt{u^2 - B^2})$
(51)	$J_{\mu - 1}(\sqrt{u^2 - B^2})$

processing application in various numbers of dimensions, we have table 4 for the required weightings, where we have specialized the values of μ . In all cases, the pattern realized is the ideal one of (34):

$$g_i(u) = J_{-\frac{1}{2}}(\sqrt{u^2 - B^2}) = \left(\frac{2}{\pi}\right)^{\frac{1}{2}} \cos(\sqrt{u^2 - B^2}) \quad \text{for all } u. \quad (52)$$

Table 4. Required Weighting for Ideal Pattern

<u>Number of Dimensions</u>	<u>Value of μ</u>	<u>Required Weighting</u>
1	$-\frac{1}{2}$	(49)
2	0	(50) with $\nu = -\frac{3}{2}$
3	$\frac{1}{2}$	(51)

The weighting given by (49) for one dimension, namely, $\mu = -1/2$, has already been presented by van der Maas [9]. However, the application of (49) to the realization of (48) for any $\mu > -1$ is new. Additionally, all the results in (50) and (51) for any $\mu > -1$, and their application to two- and three-dimensional array processing in table 4, are new. An approximation to the ideal pattern in two dimensions, namely, weighting (50) with $\nu = -1.5$, is treated in detail in appendix F.

SOME OTHER WEIGHTINGS

Another candidate class of weightings for consideration is

$$w(s) = \left(\frac{B}{\sqrt{1-s^2}} \right)^{\nu} I_{\nu}(B\sqrt{1-s^2}) = B^{2\nu} \mathcal{I}_{\nu}(B\sqrt{1-s^2}) \quad \text{for } 0 < s < 1, \quad (53)$$

of which (49) and (51) are representative examples, exclusive of the generalized functions. This class is somewhat similar in form to the earlier case in (22). Substitution of (53) in (15) yields pattern

$$g(u) = \int_0^1 ds s \left(\frac{s}{u} \right)^{\mu} J_{\mu}(us) B^{2\nu} \mathcal{I}_{\nu}(B\sqrt{1-s^2}). \quad (54)$$

This integral converges at $s = 0$ for $\mu > -1$, but needs no restriction on ν whatsoever.

To our knowledge, evaluation of (54) is not possible in closed form for general ν ; however, the following cases are evaluated in appendix G:

$$g(u) = \mathcal{J}_{\mu+1}(\sqrt{u^2 - B^2}) = \mathcal{I}_{\mu+1}(\sqrt{B^2 - u^2}) \quad \text{for } \nu = 0; \quad (55)$$

$$\begin{aligned} g(u) &= \mathcal{J}_{\mu}(\sqrt{u^2 - B^2}) - \mathcal{J}_{\mu}(u) \\ &= \mathcal{I}_{\mu}(\sqrt{B^2 - u^2}) - \mathcal{J}_{\mu}(u) \end{aligned} \quad \text{for } \nu = 1; \quad (56)$$

$$g(u) = \mathcal{J}_{\mu-1}(\sqrt{u^2 - B^2}) - \mathcal{J}_{\mu-1}(u) - \frac{1}{2} B^2 \mathcal{J}_{\mu}(u) \quad \text{for } \nu = 2. \quad (57)$$

Numerous special cases for one, two, or three dimensions are available from (55)-(57) by setting $\mu = -\frac{1}{2}$, 0, or $\frac{1}{2}$, respectively.

As an example, if we take (54) and (56) for $\nu = 1$, we have

$$\int_0^1 ds s \left(\frac{s}{u}\right)^\mu J_\mu(us) \frac{B}{\sqrt{1-s^2}} I_1(B\sqrt{1-s^2}) = J_\mu(\sqrt{u^2-B^2}) - J_\mu(u). \quad (58)$$

Addition of a δ function immediately yields, for $\mu > -1$,

$$\int_0^1 ds s \left(\frac{s}{u}\right)^\mu J_\mu(us) \left[\frac{B}{\sqrt{1-s^2}} I_1(B\sqrt{1-s^2}) + \delta(s-1) \right] = J_\mu(\sqrt{u^2-B^2}), \quad (59)$$

which has already been presented in (49) and table 3. A similar combination of (54) and (57) yields the results of (51) and the bottom entry of table 3.

Additional results for $\nu = 3, 4, \dots$ are possible via the method of appendix G.

One other two-parameter family of weightings that affords a closed form pattern is available from [10; 6.688 1], by identifying $\mu = 1$, $x = u$, $z = iB$, $\cos t = s$, and by using [5; 9.6.3 and 9.1.35]:

$$\int_0^1 ds \left(\frac{2}{\pi}\right)^{1/2} \cos(us) \frac{I_\nu(B\sqrt{1-s^2})}{\sqrt{1-s^2}} = \left(\frac{\pi}{2}\right)^{1/2} J_{\frac{\nu}{2}}\left(\frac{u+\sqrt{u^2-B^2}}{2}\right) J_{\frac{\nu}{2}}\left(\frac{u-\sqrt{u^2-B^2}}{2}\right) \text{ for } \nu > -1. \quad (60)$$

This result is restricted to the line array. The weighting is continuous at $s = 1$ if $\nu \geq 1$, and the pattern (60) decays at $3+3\nu$ dB/octave. How good this pattern is has not been pursued.

All the above results have been aimed at getting closed form results for the pattern; however, this is by no means necessary. One could consider the class of weightings (53) for any ν , or the class

$$\exp(-B^2 s^2) (1-s^2)^\nu \text{ for } 0 < s < 1 \quad (61)$$

for example, numerically by substitution in (12) or (15) and use of some integration rule like Simpson's. Once the patterns have been numerically evaluated and plotted for a sufficiently broad range of values of B and ν , good candidates can be selected at will and the corresponding weighting, (61) or (53) for example, easily evaluated. For the line array, this numerical approach is readily accomplished by use of an FFT.

DISCUSSION

The ideal pattern was defined in (34) as $(2/\pi)^{1/2} \cos(\sqrt{u^2 - B^2})$, and the corresponding weightings were given in (49)-(51). Now in the one-dimensional application, $\mu = -1/2$, van der Maas [9] has indeed shown, by taking the limit of a Dolph-Chebyshev discrete array design, that there is no pattern with a narrower mainlobe for a specified sidelobe level (and vice versa) than (34). However, strictly speaking, we have not proven that same result for the other values of μ , i.e., other numbers of dimensions. Instead, we have adopted (34) as an ideal pattern and shown that it can be realized by finite-support weighting functions with a generalized function whose singularity is centered at the edge of the array. Conceivably, there might be a different weighting that would realize a pattern that gets further into the left-lower quadrant of figure 16. However, we conjecture that this is not possible and that the leftmost curve in figure 16 is the ultimate attainable region for any weighting in any number of dimensions.

SUMMARY

We have presented a two-parameter class of Bessel weighting functions that have a closed form pattern with controllable mainlobe width, mainlobe-to-peak-sidelobe ratio, and sidelobe decay rate. These results have application to arrays in one, two, or three dimensions. In addition, the ideal pattern and the corresponding weightings required in various numbers of dimensions have been derived and presented. Where a generalized function is required, a method of approximating it has been presented and illustrated by a numerical example. Various weightings already extant in the literature were shown to be special cases or limiting cases of the general results given here.

Appendix A
DERIVATION OF RESPONSE OF PLANAR ARRAY

Let the receiving array lie in the x-y plane, and let a plane wave of wavelength λ arrive at polar angle ϕ_a and azimuthal angle θ_a ; see figure A-1. Then if the time of arrival of the plane wave at the origin is denoted

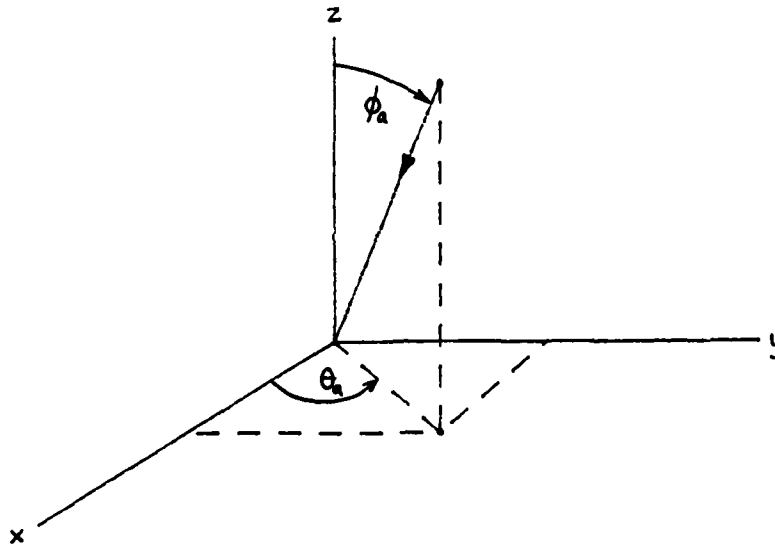


Figure A-1. Geometry for Planar Array

as 0, the time of arrival at a general point x, y in the plane of the array is

$$\tau_a = -\sin \phi_a \frac{x \cos \theta_a + y \sin \theta_a}{c}, \quad (\text{A-1})$$

where $\lambda = c/f_0$, c is the speed of propagation, and f_0 is the frequency of the plane-wave arrival.

To look in direction ϕ_l, θ_l , the receiving array should employ steering-delay

$$\tau_l = -\sin \phi_l \frac{x \cos \theta_l + y \sin \theta_l}{c} \quad (\text{A-2})$$

at the general point x, y . If, also, weighting $w_2(x, y)$ is used in the receiving array, the array output voltage response at frequency f_0 is

$$\begin{aligned} g &= \iint dx dy w_2(x, y) \exp[-i2\pi f_0(\tau_a + \tau_r)] \\ &= \iint dx dy w_2(x, y) \exp\left[-i2\pi \frac{x}{\lambda} P_1 - i2\pi \frac{y}{\lambda} P_2\right], \end{aligned} \quad (\text{A-3})$$

where we define angle functions

$$P_1 = \sin\theta_2 \cos\theta_1 - \sin\theta_1 \cos\theta_2, \quad P_2 = \sin\theta_2 \sin\theta_1 - \sin\theta_1 \sin\theta_2, \quad (\text{A-4})$$

and where the integration is carried out over all x, y where weighting $w_2 \neq 0$. Thus the planar array can have arbitrary geometry in the x, y plane; equations (A-3) and (A-4) are general results for the array response.

If weighting w_2 contains an impulse at x_0, y_0 , then we have

$$w_2(x, y) = \delta(x - x_0) \delta(y - y_0), \quad (\text{A-5})$$

with array response

$$g = \exp\left[-i2\pi \frac{x_0}{\lambda} P_1 - i2\pi \frac{y_0}{\lambda} P_2\right], \quad (\text{A-6})$$

which never decays in amplitude with increasing angle.

SPECIALIZATION TO CIRCULAR ARRAY

As a special case of the above, consider a planar-circular array of radius R with weighting independent of angle; i.e.,

$$w_2(x, y) = \begin{cases} w_1(\sqrt{x^2 + y^2}) & \text{for } x^2 + y^2 < R^2 \\ 0 & \text{otherwise} \end{cases}. \quad (\text{A-7})$$

Then response (A-3) becomes

$$\begin{aligned}
 g &= \int_0^R dr r \int_{-\pi}^{\pi} d\theta w_1(r) \exp \left[-i2\pi \frac{r}{\lambda} (P_1 \cos\theta + P_2 \sin\theta) \right] \\
 &= 2\pi \int_0^R dr r w_1(r) J_0 \left(2\pi \frac{r}{\lambda} \sqrt{P_1^2 + P_2^2} \right). \tag{A-8}
 \end{aligned}$$

And from (A-4), we have

$$\begin{aligned}
 \sqrt{P_1^2 + P_2^2} &= \left[\sin^2 \theta_2 + \sin^2 \theta_a - 2 \sin \theta_2 \sin \theta_a \cos(\theta_2 - \theta_a) \right]^{1/2} \\
 &= \left| \sin \theta_2 e^{i\theta_2} - \sin \theta_a e^{i\theta_a} \right|. \tag{A-9}
 \end{aligned}$$

Now let

$$r = Rs \tag{A-10}$$

in (A-8). There follows, for response (A-8),

$$g(u) = \int_0^1 ds s J_0(us) w(s), \tag{A-11}$$

where

$$u = 2\pi \frac{R}{\lambda} \left| \sin \theta_2 e^{i\theta_2} - \sin \theta_a e^{i\theta_a} \right|, \tag{A-12}$$

and

$$w(s) = 2\pi R^2 w_1(Rs) \quad \text{for } 0 < s < 1. \tag{A-13}$$

Thus the voltage response $g(u)$ is given by a zero-th order Bessel transform over $(0,1)$ of normalized weighting $w(s)$. Dimensionless parameter u incorporates the received wavelength λ , the array radius R , and the various look and arrival angles.

Appendix B
DERIVATION OF RESPONSE OF VOLUMETRIC ARRAY

Consider a plane wave of wavelength λ arriving at angles θ_a, ϕ_a ; see figure A-1. The time of arrival (relative to the origin) at a general point x, y, z in the volumetric array is [11; eq. 3]

$$\tau_a = -\frac{1}{c} [x \cos \theta_a \sin \phi_a + y \sin \theta_a \sin \phi_a + z \cos \phi_a]. \quad (B-1)$$

To look in direction θ_2, ϕ_2 , the delay used at location x, y, z should be

$$\tau_2 = \frac{1}{c} [x \cos \theta_2 \sin \phi_2 + y \sin \theta_2 \sin \phi_2 + z \cos \phi_2]. \quad (B-2)$$

The response of a weighted array, at frequency f_0 , is then

$$\begin{aligned} g &= \iiint dx dy dz w_3(x, y, z) \exp [-i2\pi f_0 (\tau_a + \tau_2)] \\ &= \iiint dx dy dz w_3(x, y, z) \exp \left[-i\frac{2\pi}{\lambda} (xP_1 + yP_2 + zP_3) \right], \end{aligned} \quad (B-3)$$

where w_3 is the weighting and

$$\begin{aligned} P_1 &= \cos \theta_2 \sin \phi_2 - \cos \theta_a \sin \phi_a, \\ P_2 &= \sin \theta_2 \sin \phi_2 - \sin \theta_a \sin \phi_a, \\ P_3 &= \cos \phi_2 - \cos \phi_a. \end{aligned} \quad (B-4)$$

The integration in (B-3) is over all x, y, z where $w_3 \neq 0$. (B-3) is the general result for any time-delay steered volumetric array.

SPECIALIZATION TO SPHERICAL ARRAY

Let weighting w_3 depend only on the distance from the array center; that is,

$$w_3(x,y,z) = w_1\left(\sqrt{x^2+y^2+z^2}\right) \text{ for } x^2+y^2+z^2 < R^2, \quad (B-5)$$

where R is the sphere radius. Then the voltage response of the array is, from (B-3) and (B-5),

$$\begin{aligned} g &= \iiint_R dx dy dz w_1\left(\sqrt{x^2+y^2+z^2}\right) \exp\left[-i\frac{2\pi}{\lambda}(xP_1+yP_2+zP_3)\right] \\ &= \int_0^R dr r^2 \int_0^\pi d\theta \sin\theta \int_{-\pi}^\pi d\phi w_1(r) \exp\left[-i2\pi\frac{r}{\lambda}(P_1\cos\theta \sin\phi + P_2\sin\theta \sin\phi + P_3\cos\theta)\right] \\ &= 2\pi \int_0^R dr r^2 w_1(r) \int_0^\pi d\theta \sin\theta \exp\left(-i2\pi\frac{r}{\lambda} P_3\cos\theta\right) J_0\left(2\pi\frac{r}{\lambda} \sqrt{P_1^2+P_2^2} \sin\theta\right), \quad (B-6) \end{aligned}$$

where we have changed to polar coordinates.

In the integral on θ , let $t = \cos \theta$; the inner integral in (B-6) becomes, by use of [10; 6.677 6],

$$\begin{aligned} &\int_{-1}^1 dt \exp\left(-i2\pi\frac{r}{\lambda} P_3 t\right) J_0\left(2\pi\frac{r}{\lambda} \sqrt{P_1^2+P_2^2} \sqrt{1-t^2}\right) \\ &= 2 \int_0^1 dt \cos\left(2\pi\frac{r}{\lambda} P_3 t\right) J_0\left(2\pi\frac{r}{\lambda} \sqrt{P_1^2+P_2^2} \sqrt{1-t^2}\right) \\ &= 2 \frac{\sin\left(2\pi\frac{r}{\lambda} Q\right)}{2\pi\frac{r}{\lambda} Q}, \quad (B-7) \end{aligned}$$

where we define

$$Q \equiv \sqrt{p_1^2 + p_2^2 + p_3^2}. \quad (B-8)$$

Then the response is, upon substitution of (B-7) in (B-6),

$$g = 4\pi \int_0^R dr r^2 w_1(r) \frac{\sin\left(2\pi \frac{r}{\lambda} Q\right)}{2\pi \frac{r}{\lambda} Q}. \quad (B-9)$$

Now let $r = Rs$; then the response can be written as

$$g(u) = \int_0^1 ds \left(\frac{2}{\pi}\right)^{1/2} s \frac{\sin(us)}{u} w(s), \quad (B-10)$$

where

$$w(s) \equiv (2\pi)^{3/2} R^3 w_1(Rs), \quad (B-11)$$

and dimensionless parameter

$$u \equiv 2\pi \frac{R}{\lambda} Q. \quad (B-12)$$

The quantity Q , involving the look and arrival angles, can be expressed as

$$Q = \left[2 - 2 \cos \theta_\lambda \cos \theta_a - 2 \sin \theta_\lambda \sin \theta_a \cos(\theta_\lambda - \theta_a) \right]^{1/2} \quad (B-13)$$

Thus the general result, (B-10), for the volumetric array is given by a sine transform of the normalized weighting w .

Appendix C
MONOTONICITY OF BESSEL WEIGHTING

We investigate here the behavior of weighting (22):

$$w(s) = \left(\frac{\sqrt{1-s^2}}{B} \right)^v I_v \left(B \sqrt{1-s^2} \right) \quad \text{for } 0 < s < 1. \quad (\text{C-1})$$

Let $y = B \sqrt{1-s^2}$; then (C-1) becomes

$$w(s) = B^{-2v} y^v I_v(y). \quad (\text{C-2})$$

Now [5; 9.6.28]

$$\frac{d}{dy} \left\{ y^v I_v(y) \right\} = y^v I_{v-1}(y), \quad (\text{C-3})$$

which is positive for $v \geq 0$, $y > 0$; see, for example, [5; 9.6.10]. Thus (C-2) is monotonically increasing in y if $v \geq 0$; therefore (C-1) is monotonically decreasing in s if $v \geq 0$.

Appendix D
PROGRAM FOR CALCULATION OF PATTERN (28)

```

10   Alpha=-.5
20   PLOTTER IS "9872A"
30   LIMIT 25,175,35,245
40   OUTPUT 705;"VSS"
50   SCALE 0.6*PI,-70,0
60   GRID F1,10
70   PENUP
80   FOR B=2 TO 8 STEP 2
90   B2=B*B
100  F=FNInu<nu>(Alpha,B)
110  FOR U=0 TO B STEP .05
120  Y=FNInu<nu>(Alpha,SQR(B2-U*U))
130  PLOT U,20*LGT(ABS(Y/F))
140  NEXT U
150  FOR U=B TO 6*PI STEP .05
160  Y=FNJnu<nu>(Alpha,SQR(U*U-B2))
170  PLOT U,20*LGT(ABS(Y/F))
180  NEXT U
190  PENUP
200  NEXT B
210  END
220  !
230  DEF FNGamma(X) = GAMMA(X)  via HART, page 275, #5231
240  N=INT(X)
250  R=X-N
260  IF (N=0) OR (R<>0) THEN 290
270  PRINT "FNGamma(X) IS NOT DEFINED FOR X = ";X
280  STOP
290  IF R>0 THEN 320
300  Gamma2=1
310  GOTO 360
320  P=3.36954359131+R*(1.09850630453+R*(1.142928807949+R*(3.93013464186E-2)))
330  P=43.9410209189+R*(22.9680800836+R*(12.8021598112+R*P))
340  Q=43.9410209191+R*(4.39050474596-R*(7.15075063299-R))
350  Gamma2=P/Q          ! GAMMA(2+R) for 0 < R < 1
360  IF N>2 THEN 400
370  IF N<2 THEN 450
380  Gamma=Gamma2
390  GOTO 500
400  Gamma=Gamma2
410  FOR K=1 TO N-2
420  Gamma=Gamma*(X-K)
430  NEXT K
440  GOTO 500
450  R=1
460  FOR K=0 TO 1-N
470  R=R*(X+K)
480  NEXT K
490  Gamma=Gamma2/R
500  RETURN Gamma
510  FNEND
520  !

```

TR 6761

```

530 DEF FNJnu(x) (Nu, X) ! Jnu(X) via 9.4.1
540 IF ABS(X) < 1 THEN 550
550 A = .797884560883
560 IF Nu = 0 THEN RETURN FNJo(X)
570 IF Nu = .5 THEN RETURN A * SIN(X) / X
580 IF Nu = -.5 THEN RETURN A * COS(X)
590 IF Nu = 1 THEN RETURN FNJ1(X) / X
600 IF Nu = -1 THEN RETURN -FNJ1(X) / X
610 IF Nu = 1.5 THEN RETURN A * (SIN(X) - X * COS(X)) / X ** 3
620 IF Nu = -1.5 THEN RETURN -A * (X * SIN(X) + COS(X))
630 IF Nu = 2 THEN RETURN (2 * FNJ1(X) - X * FNJo(X)) / X ** 3
640 IF Nu = -2 THEN RETURN (2 * FNJ1(X) - X * FNJo(X)) / X
650 R = Nu
660 IF (INT(R) <> R) OR (R) = 0 THEN 680
670 K = R - Nu
680 S = T = 1 / (2 * R * FNGamma(R + 1))
690 R = -.25 * X * X
700 Big = ABS(S)
710 FOR N = 1 TO 100
720 T = T * R / (N * (N + R))
730 S = S + T
740 Big = MAX(Big, ABS(S))
750 IF ABS(T) <= 1E-11 + ABS(S) THEN 790
760 NEXT N
770 PRINT "100 TERMS IN FNJnu(x)(Nu, X) AT " ! Nu ! X
780 PAUSE
790 D = 12 - LGT(ABS(Big / S)) ! NO. OF SIGNIF. DIGITS
800 IF K > 0 THEN S = S + (4 * R) ^ K
810 RETURN S
820 FNEND
830 !
840 DEF FNJo(X) ! Jo(X) via 9.4.1 & 9.4.3 of AMS 55
850 Y = ABS(X)
860 IF Y > 3 THEN 910
870 T = Y * Y / 9
880 Jo = .04444479 - T * (.0039444 - T * .00021)
890 Jo = 1 - T * (.2499997 - T * (.12656208 - T * (.3163366 - T * Jo)))
900 GOTO 970
910 T = 3 / Y
920 Jo = 9.512E-5 - T * (.00137237 - T * (.00072805 - T * .00014476))
930 Jo = .79788456 - T * (.7E-7 + T * (.00552740 + T * Jo))
940 S = .00262573 - T * (.00054125 + T * (.00029333 - T * .00013558))
950 T = Y - .78539816 - T * (.04166397 + T * (.954E-5 - T * S))
960 Jo = Jo * COS(T / SQR(Y))
970 RETURN Jo
980 FNEND
990 !
1000 DEF FNJ1(X) ! J1(X) via 9.4.4 & 9.4.6 of AMS 55
1010 Y = ABS(X)
1020 IF Y > 3 THEN 1070
1030 T = Y * Y / 9
1040 J1 = .00443319 - T * (.00031761 - T * .00001109)
1050 J1 = X * (.5 - T * (.56249985 - T * (.21093573 - T * (.00354289 - T * J1))))
1060 GOTO 1130
1070 T = 3 / Y
1080 J1 = .00017105 - T * (.00249511 - T * (.00113653 - T * .00020022))
1090 J1 = .79788456 + T * (.156E-6 + T * (.01659667 + T * J1))
1100 S = .00637879 - T * (.00074348 + T * (.00079824 - T * .00029166))
1110 T = Y - 2.35613449 + T * (.12499612 + T * (.5.65E-5 - T * S))
1120 J1 = SGN(X) * J1 * COS(T / SQR(Y))
1130 RETURN J1
1140 FNEND
1150 !

```

```

1160 DEF FNInuxnu(Nu,X)      ! In(x) via 9.8.1 & 9.8.2
1170 IF ABS(X)>.1 THEN 1290
1180 A=.398942280401
1190 E=EXP(X)
1200 IF Nu=0 THEN RETURN FNIO(X)
1210 IF Nu=.5 THEN RETURN A*(E-1)/E/X
1220 IF Nu=-.5 THEN RETURN A*(E+1)/E
1230 IF Nu=1 THEN RETURN FNII(X)/X
1240 IF Nu=-1 THEN RETURN FNII(X)*X
1250 IF Nu=1.5 THEN RETURN A*(X-1)*E+(X+1)*E/X+3
1260 IF Nu=-1.5 THEN RETURN A*(X-1)*E-(X+1)*E
1270 IF Nu=2 THEN RETURN (X+FNIO(X))-2*FNII(X)+X+3
1280 IF Nu=-2 THEN RETURN (X+FNIO(X))-2*FNII(X)+X
1290 A=Nu
1300 IF (INT(A)/>A) OR (A>=0) THEN 1320
1310 K=A--Nu
1320 S=T=1/(2^A*FNGamma(A+1))
1330 R=.25*X*X
1340 Big=ABS(S)
1350 FOR N=1 TO 100
1360 T=T*R/(N*(N+A))
1370 S=S+T
1380 Big=MAX(Big,ABS(S))
1390 IF ABS(T)<=1E-11+ABS(S) THEN 1430
1400 NEXT N
1410 PRINT "100 TERMS IN FNInuxnu(Nu,X) AT ";Nu;X
1420 PAUSE
1430 D=12-LGT(ABS(Big/S)) ! NO. OF SIGNIF. DIGITS
1440 IF K>0 THEN S=S*(4*R)^K
1450 RETURN S
1460 FNEND
1470 !
1480 DEF FNIO(X)      ! IO(X) via 9.8.1 & 9.8.2
1490 Y=ABS(X)
1500 IF Y>3.75 THEN 1550
1510 T=Y+Y/14.0625
1520 Io=.2659732+T*(.0360768+T*(.0045813))
1530 Io=1+T*(3.5156229+T*(3.0899424+T*(1.2067452+T*(Io))))
1540 GOTO 1590
1550 T=3.75/Y
1560 Io=.00916281-T*(.02057706-T*(.02635537-T*(.01647633-T*(.00392377))))
1570 Io=.39894228+T*(.01328592+T*(.00225319-T*(.00157565-T*(Io))))
1580 Io=Io*EXP(Y)/SQR(Y)
1590 RETURN Io
1600 FNEND
1610 !
1620 DEF FNII(X)      ! II(X) via 9.8.3 & 9.8.4
1630 Y=ABS(X)
1640 IF Y>3.75 THEN 1690
1650 T=Y+Y/14.0625
1660 I1=.02658733+T*(.00201532+T*(.00032411))
1670 I1=X*(.5+T*(.87890594+T*(.51498869+T*(.15084934+T*(I1))))
1680 GOTO 1730
1690 T=3.75/Y
1700 I1=.01031555-T*(.02282967-T*(.02895312-T*(.01737654-T*(.00420059))))
1710 I1=.39894228-T*(.03988024+T*(.00362018-T*(.00163801-T*(I1))))
1720 I1=SGN(X)+I1*EXP(Y)/SQR(Y)
1730 RETURN I1
1740 FNEND

```

Appendix E
DERIVATION OF WEIGHTING FOR IDEAL PATTERN

We want to realize pattern (23),

$$g(u) = \int_{u+v+1}^{\infty} \sqrt{u^2 - B^2} \quad \text{for all } u, \quad (\text{E-1})$$

for any $u > -1$, but without the restriction $v > -1$, which was required for convergence of integral (22). $J_\alpha(z)$ was defined in (17) et seq.

We begin the derivation for the required weighting to realize (E-1) by substituting (E-1) in (16):

$$w(s) = \int_0^{\infty} du u \left(\frac{u}{s}\right)^\mu J_\mu(su) \int_{u+v+1}^{\infty} \sqrt{u^2 - B^2} \quad \text{for } s > 0. \quad (\text{E-2})$$

It is important to observe that we must allow all $s > 0$ in (E-2); hopefully, when we evaluate $w(s)$ from (E-2), it will be zero for $s > 1$.

Now we already know from (22) and (23) that (E-2) yields

$$w(s) = \begin{cases} \left(\frac{\sqrt{1-s^2}}{B}\right)^\nu I_\nu(B\sqrt{1-s^2}) & \text{for } 0 < s < 1 \\ 0 & \text{for } 1 < s \end{cases} \quad \text{if } \mu > -1, \nu > -1. \quad (\text{E-3})$$

Letting $\alpha = \mu + \nu + 1$ in (E-2) and (E-3), and eliminating ν , we have the useful integral identity

$$\int_0^{\infty} du u \left(\frac{u}{s}\right)^\mu J_\mu(su) \int_\alpha^{\infty} \sqrt{u^2 - B^2} = \begin{cases} \left(\frac{\sqrt{1-s^2}}{B}\right)^{\alpha-\mu-1} I_{\alpha-\mu-1}(B\sqrt{1-s^2}) & \text{for } 0 < s < 1 \\ 0 & \text{for } 1 < s \end{cases} \quad (\text{E-4})$$

For convergence of this integral at $u = 0$, we require $\mu > -1$, whereas for convergence at $u = \infty$, we must have $\alpha > \mu$; i.e., $-1 < \mu < \alpha$.

Now we have the relation [5; 9.1.30]

$$u\left(\frac{u}{s}\right)^\mu J_\mu(su) = -\frac{1}{s} \frac{d}{ds} \left\{ u\left(\frac{u}{s}\right)^{\mu-1} J_{\mu-1}(su) \right\} \quad \text{for } s > 0. \quad (\text{E-5})$$

Thus (E-2) can be expressed as

$$w(s) = -\frac{1}{s} \frac{d}{ds} \left\{ \int_0^\infty du u\left(\frac{u}{s}\right)^{\mu-1} J_{\mu-1}(su) J_{\nu+1}\left(\sqrt{u^2 - B^2}\right) \right\} \quad \text{for } s > 0. \quad (\text{E-6})$$

Appeal to (E-4) now reveals that

$$w(s) = \left\{ \begin{array}{ll} -\frac{1}{s} \frac{d}{ds} \left\{ \left(\frac{\sqrt{1-s^2}}{B}\right)^{\nu+1} I_{\nu+1}\left(B\sqrt{1-s^2}\right) \right\} & \text{for } 0 < s < 1 \\ 0 & \text{for } 1 < s \end{array} \right\}, \quad (\text{E-7})$$

provided that $\mu > 0$, $\nu > -2$.

We have succeeded in extending the range of ν from $\nu > -1$ to $\nu > -2$, as desired, but have apparently altered and restricted the range of μ from $\mu > -1$ to $\mu > 0$. However, this last restriction is due solely to the method of derivation, and may be restored to $\mu > -1$, by observing that the right-hand side of (E-7) is analytic in μ (in fact, constant), and that the function $w(s)$ defined by (E-2) is analytic* in μ for $\mu > -1$. Thus (E-7) gives the required weighting to realize pattern (E-1), provided that

$$\mu > -1, \nu > -2. \quad (\text{E-8})$$

However, care must be taken, in the evaluation of the derivative in (E-7), to account for any generalized functions that may be generated.

* We are using the fact that $J_\alpha(z)$ is an entire function of α , regardless of the value of z ; see (17) et seq.

In (E-7), define the function

$$w_1(s) = \left\{ \begin{array}{ll} \left(\frac{\sqrt{1-s^2}}{B}\right)^{\nu+1} I_{\nu+1}(B\sqrt{1-s^2}) & \text{for } 0 < s < 1 \\ 0 & \text{for } 1 < s \end{array} \right\}. \quad (\text{E-9})$$

Then there follows

$$w(s) = -\frac{1}{s} \frac{d}{ds} w_1(s) \quad \text{for all } s, \quad \text{if } \mu > -1, \nu > -2. \quad (\text{E-10})$$

We now break the region $\nu > -2$ into the three subcases (i) $\nu > -1$,
(ii) $\nu = -1$, (iii) $-2 < \nu < -1$.

(i) $\nu > -1$

As $s \rightarrow 1^-$, $w_1(s)$ in (E-9) approaches 0, since $\nu+1 > 0$. Thus $w_1(s)$ in (E-9) is continuous for all s , and we find, by the use of [5; 9.6.28] in (E-7), that

$$w(s) = \left\{ \begin{array}{ll} \left(\frac{\sqrt{1-s^2}}{B}\right)^{\nu} I_{\nu}(B\sqrt{1-s^2}) & \text{for } 0 < s < 1 \\ 0 & \text{for } 1 < s \end{array} \right\}, \quad (\text{E-11})$$

which checks (22), as it must of course, for $\nu > -1$.

We observe that

$$w(s) \sim \frac{(1-s)^{\nu}}{\Gamma(\nu+1)} \quad \text{as } s \rightarrow 1^-. \quad (\text{E-12})$$

Thus for $-1 < \nu < 0$, there is an integrable singularity in $w(s)$ at $s = 1$. For $\nu > 0$, $w(s)$ is continuous at $s = 1$, while for $\nu = 0$, $w(s)$ has a discontinuous step of value -1 at $s = 1$.

(ii) $\nu = -1$

Now, from (E-9),

$$w_1(s) = \left\{ \begin{array}{ll} I_0(B\sqrt{1-s^2}) & \text{for } 0 < s < 1 \\ 0 & \text{for } 1 < s \end{array} \right\}. \quad (\text{E-13})$$

This function has a discontinuous step of value -1 at $s = 1$. Thus, from (E-10) and [5; 9.6.28 and 9.6.6],

$$\begin{aligned} w(s) &= \left\{ \begin{array}{ll} \frac{B}{\sqrt{1-s^2}} I_{-1}(B\sqrt{1-s^2}) + \delta(s-1) & \text{for } 0 \leq s \leq 1 \\ 0 & \text{for } 1 < s \end{array} \right\} \\ &= \left\{ \begin{array}{ll} \frac{B}{\sqrt{1-s^2}} I_1(B\sqrt{1-s^2}) + \delta(s-1) & \text{for } 0 \leq s \leq 1 \\ 0 & \text{for } 1 < s \end{array} \right\}. \end{aligned} \quad (\text{E-14})$$

The Bessel function portion of this weighting approaches the finite value $B^2/2$ as $s \rightarrow 1^-$. The integrable singularity at $s = 1$ of the previous subcase for $\nu > -1$ has evolved here into a δ -function for $\nu = -1$ at $s = 1$.

This weighting $w(s)$ in (E-14) realizes the desired pattern in (E-1) for $\nu = -1$, namely,

$$J_{\mu}(\sqrt{u^2 - B^2}) \quad \text{for } \mu > -1. \quad (\text{E-15})$$

The special case of a linear array, $\mu = -1/2$, yields the ideal pattern

$$J_{-1/2}(\sqrt{u^2 - B^2}) = \left(\frac{2}{\pi}\right)^{1/2} \cos(\sqrt{u^2 - B^2}). \quad (\text{E-16})$$

This weighting-pattern pair, (E-14) and (E-16), is already known for the line array under the name of van der Maas [9].

An alternative way of obtaining the result (E-14) is by taking the limit of (E-11) as $\nu \rightarrow -1$. First we observe that

$$\lim_{\nu \rightarrow -1} \left(\frac{\sqrt{1-s^2}}{B} \right)^\nu I_\nu \left(B \sqrt{1-s^2} \right) = \frac{B}{\sqrt{1-s^2}} I_{-1} \left(B \sqrt{1-s^2} \right) \text{ for } s < 1, \quad (\text{E-17})$$

since $I_\nu(z)$ is an entire function of ν when $z \neq 0$ [5; 9.6.1]. We then define a difference or remainder function (for $\nu > -1$) as

$$R_\nu(s) \equiv \left(\frac{\sqrt{1-s^2}}{B} \right)^\nu I_\nu \left(B \sqrt{1-s^2} \right) - \frac{B}{\sqrt{1-s^2}} I_1 \left(B \sqrt{1-s^2} \right) \text{ for } s < 1, \quad (\text{E-18})$$

where we used [5; 9.6.6]. The area under the remainder function $s R_\nu(s)$ in a small region near $s = 1$ is

$$\begin{aligned} \int_{1-\epsilon}^1 ds s R_\nu(s) &= \int_0^{(2\epsilon-\epsilon^2)^{1/2}} dt \left[t \left(\frac{t}{B} \right)^\nu I_\nu(Bt) - B I_1(Bt) \right] \\ &= \left(\frac{\sqrt{2\epsilon-\epsilon^2}}{B} \right)^{\nu+1} I_{\nu+1} \left(B \sqrt{2\epsilon-\epsilon^2} \right) - I_0 \left(B \sqrt{2\epsilon-\epsilon^2} \right) + 1 \text{ for } \nu > -1, \end{aligned} \quad (\text{E-19})$$

where we used [5; 9.6.28]. Therefore,

$$\lim_{\nu \rightarrow -1} \int_{1-\epsilon}^1 ds s R_\nu(s) = 1, \text{ regardless of } \epsilon (>0). \quad (\text{E-20})$$

Thus since factor s is 1 at the upper limit of integration,

$$\lim_{\nu \rightarrow -1} R_\nu(s) = \delta(s-1). \quad (\text{E-21})$$

Therefore, combining (E-17) and (E-21), we obtain

$$\lim_{\nu \rightarrow -1} \left(\frac{\sqrt{1-s^2}}{B} \right)^\nu I_\nu \left(B \sqrt{1-s^2} \right) = \frac{B}{\sqrt{1-s^2}} I_1 \left(B \sqrt{1-s^2} \right) + \int (s-1) \quad \text{for } s \leq 1, \quad (\text{E-22})$$

in agreement with (E-14).

An alternative and simpler equivalent form of (E-22) is

$$\lim_{\nu \rightarrow -1} (\sqrt{s})^\nu I_\nu (\sqrt{s}) = \frac{I_1(\sqrt{s})}{\sqrt{s}} + 2\int(s) \quad \text{for } s \geq 0. \quad (\text{E-23})$$

The derivation of (E-23) is similar to that given above in (E-18)-(E-21).

(iii) $-2 < \nu < -1$

We return to (E-7) and (E-9). Observe that [5; 9.6.7]

$$w_1(s) \sim \frac{(1-s^2)^{\nu+1}}{2^{\nu+1} \Gamma(\nu+2)} \quad \text{as } s \rightarrow 1-. \quad (\text{E-24})$$

Since we now have

$$-1 < \nu+1 < 0, \quad (\text{E-25})$$

there is an integrable singularity in $w_1(s)$ at $s = 1$. Thus the derivative in (E-10) will generate a generalized function with a singularity located at $s = 1$. We handle this case by defining an auxiliary function

$$A(s) \equiv \left\{ \begin{array}{ll} \frac{(1-s^2)^{\nu+1}}{2^{\nu+1} \Gamma(\nu+2)} & \text{for } 0 < s < 1 \\ 0 & \text{for } 1 < s \end{array} \right\}. \quad (\text{E-26})$$

Then using (E-9), the difference

$$w_1(s) - A(s) = \begin{cases} \left(\frac{\sqrt{1-s^2}}{B}\right)^{\nu+1} I_{\nu+1}(B\sqrt{1-s^2}) - \frac{(1-s^2)^{\nu+1}}{2^{\nu+1}\Gamma(\nu+2)} & \text{for } 0 < s < 1 \\ 0 & \text{for } 1 < s \end{cases} \quad (\text{E-27})$$

is a continuous function of s ; in fact,

$$w_1(s) - A(s) \sim \frac{B^2(1-s^2)^{\nu+2}}{2^{\nu+3}\Gamma(\nu+3)} \quad \text{as } s \rightarrow 1-, \quad (\text{E-28})$$

which approaches zero since $\nu > -2$. Therefore, the required weighting $w(s)$ in (E-10) can be expressed as

$$\begin{aligned} w(s) &= -\frac{1}{s} \frac{d}{ds} \left\{ w_1(s) - A(s) + A(s) \right\} \\ &= \left[\left(\frac{\sqrt{1-s^2}}{B}\right)^{\nu} I_{\nu}(B\sqrt{1-s^2}) - \frac{(1-s^2)^{\nu}}{2^{\nu}\Gamma(\nu+1)} \right] - \frac{1}{s} \frac{d}{ds} A(s) \\ &\equiv D(s) + G(s), \end{aligned} \quad (\text{E-29})$$

where both $D(s)$ and $G(s)$ are zero for $1 < s$. The difference function $D(s)$ possesses an integrable singularity at $s = 1$; in fact (recall (E-25)),

$$D(s) \sim \frac{B^2(1-s^2)^{\nu+1}}{2^{\nu+2}\Gamma(\nu+2)} \quad \text{as } s \rightarrow 1-. \quad (\text{E-30})$$

The last term in $w(s)$ in (E-29) is a generalized function; from (E-26),

$$\begin{aligned}
G(s) &= -\frac{1}{s} \frac{d}{ds} A(s) \\
&= -\frac{1}{2^{\nu+1} \Gamma(\nu+2)} \frac{1}{s} \frac{d}{ds} \left\{ (1-s^2)^{\nu+1} U(1-s^2) \right\} \\
&= \frac{(1-s^2)^\nu}{2^\nu \Gamma(\nu+1)} U(1-s^2) \Big|_G \quad \text{for } s > 0,
\end{aligned} \tag{E-31}$$

where the sub G denotes a generalized function. Here step function

$$U(t) = \begin{cases} 0 & \text{for } t < 0 \\ 1 & \text{for } t > 0 \end{cases}. \tag{E-32}$$

Combining (E-29) and (E-31), the required weighting is

$$w(s) = \begin{cases} \left(\frac{\sqrt{1-s^2}}{B} \right)^\nu I_\nu(B\sqrt{1-s^2}) - \frac{(1-s^2)^\nu}{2^\nu \Gamma(\nu+1)} + \frac{(1-s^2)^\nu}{2^\nu \Gamma(\nu+1)} \Big|_G & \text{for } 0 < s < 1 \\ 0 & \text{for } 1 < s \end{cases}. \tag{E-33}$$

We have now completed the consideration of the three subcases delineated under (E-10). We now wish to extend ν to values that are equal to and less than -2 , so that we can handle the volumetric array discussed in (37) et seq.

We return to (E-6) and employ (E-5) again:

$$\begin{aligned}
w(s) &= -\frac{1}{s} \frac{d}{ds} \left\{ \int_0^\infty du \left[-\frac{1}{s} \frac{d}{ds} \left\{ u \left(\frac{u}{s} \right)^{\nu-2} J_{\nu-2}(su) \right\} \right] J_{\nu+1}(\sqrt{u^2-B^2}) \right\} \\
&= -\frac{1}{s} \frac{d}{ds} \left\{ -\frac{1}{s} \frac{d}{ds} \int_0^\infty du u \left(\frac{u}{s} \right)^{\nu-2} J_{\nu-2}(su) J_{\nu+1}(\sqrt{u^2-B^2}) \right\} \quad \text{for } s > 0.
\end{aligned} \tag{E-34}$$

Recourse to (E-4) yields

$$w(s) = \begin{cases} -\frac{1}{s} \frac{d}{ds} \left\{ -\frac{1}{s} \frac{d}{ds} \left[\left(\frac{\sqrt{1-s^2}}{B} \right)^{\nu+2} I_{\nu+2}(B\sqrt{1-s^2}) \right] \right\} & \text{for } 0 < s < 1 \\ 0 & \text{for } 1 < s \end{cases} \quad (\text{E-35})$$

provided that $\nu > -3$, $\mu > 1$. However, the last restriction on μ may be restored to $\mu > -1$, by the argument under (E-7). Thus (E-35) gives the required weighting to realize pattern (E-1), provided that

$$\mu > -1, \nu > -3. \quad (\text{E-36})$$

The only subcase of (E-35) that we consider in detail is:

(iv) $\nu = -2$

We now can write (E-35) as

$$w(s) = -\frac{1}{s} \frac{d}{ds} \left\{ -\frac{1}{s} \frac{d}{ds} \left\{ I_0(B\sqrt{1-s^2}) U(1-s) \right\} \right\}. \quad (\text{E-37})$$

Then [5; 9.6.27]

$$\begin{aligned} & -\frac{1}{s} \frac{d}{ds} \left\{ I_0(B\sqrt{1-s^2}) U(1-s) \right\} \\ &= -\frac{1}{s} I_1(B\sqrt{1-s^2}) B \frac{1}{2} (1-s^2)^{-\frac{1}{2}} (-2s) U(1-s) - \frac{1}{s} I_0(0) [-\delta(s-1)] \\ &= \frac{B}{\sqrt{1-s^2}} I_1(B\sqrt{1-s^2}) U(1-s) + \delta(s-1). \end{aligned} \quad (\text{E-38})$$

Therefore [5; 9.6.28],

$$\begin{aligned}
 w(s) &= -\frac{1}{s} \frac{d}{ds} \left\{ \frac{B}{\sqrt{1-s^2}} I_1(B\sqrt{1-s^2}) U(1-s) + \delta(s-1) \right\} \\
 &= -\frac{B^2}{s} \frac{d}{ds} \left\{ U(B\sqrt{1-s^2}) U(1-s) \right\} - \delta(s-1) - \delta'(s-1) \\
 &= \frac{B^2}{1-s^2} I_2(B\sqrt{1-s^2}) U(1-s) + \left(\frac{B^2}{2} - 1 \right) \delta(s-1) - \delta'(s-1).
 \end{aligned}
 \tag{E-39}$$

Here we have used (21) and

$$\frac{1}{s} \delta'(s-1) = \delta(s-1) + \delta'(s-1),
 \tag{E-40}$$

which follows from

$$\begin{aligned}
 f(x) \delta'(x-a) &= \left[f(a) + f'(a)(x-a) + O\{(x-a)^2\} \right] \delta'(x-a) \\
 &= f(a) \delta'(x-a) - f'(a) \delta(x-a).
 \end{aligned}
 \tag{E-41}$$

This required weighting, (E-39) for $\nu = -2$, has both a δ function and a δ' function at $s = 1$.

Summary

The required weightings to realize pattern (E-1) are given by

$$\left. \begin{array}{l}
 \text{(E-11) for } \nu > -1 \\
 \text{(E-14) for } \nu = -1 \\
 \text{(E-33) for } -2 < \nu < -1 \\
 \text{(E-39) for } \nu = -2 \\
 \text{(E-35) for } -3 < \nu < -2
 \end{array} \right\} \text{ for } \mu > -1.
 \tag{E-42}$$

Appendix F
APPROXIMATION OF A GENERALIZED FUNCTION

Equation (50) or (E-33) gives the required weighting, for $-2 < \nu < -1$, to realize pattern (48) in terms of a generalized function which is difficult to interpret. Here we address this interpretation by means of an approximation to the generalized function (E-31). We begin by approximating the (singular) auxiliary function $A(s)$ defined in (E-26) by an ordinary function $A_\epsilon(s)$, and then derive an approximation to generalized function $G(s)$ of (E-31) according to the same rule, namely,

$$G_\epsilon(s) = -\frac{1}{s} \frac{d}{ds} A_\epsilon(s). \quad (F-1)$$

In particular, consider $A_\epsilon(s)$ as shown in figure F-1; that is, $A_\epsilon(s)$ is still given by (E-26) for $0 \leq s \leq 1-\epsilon$, but then tapers linearly to zero at $s = 1$ in order to be everywhere continuous. The height H of $A_\epsilon(s)$ at $s = 1-\epsilon$ is, from (E-26),

$$H = \frac{\epsilon^{\nu+1} (1-\epsilon/2)^{\nu+1}}{\Gamma(\nu+2)} \quad (> 0). \quad (F-2)$$

For small ϵ , we have

$$H \sim \frac{\epsilon^{\nu+1}}{\Gamma(\nu+2)} \quad \text{as } \epsilon \rightarrow 0+, \quad (F-3)$$

which tends to $+\infty$ as $\epsilon \rightarrow 0+$, since we have, from (E-25),

$$-1 < \nu+1 < 0. \quad (F-4)$$

The result of applying (F-1) to figure F-1 is shown in figure F-2. The large positive pulse in $(1-\epsilon, 1)$ has height proportional to

$$\frac{H}{\epsilon} = \frac{\epsilon^\nu (1-\epsilon/2)^{\nu+1}}{\Gamma(\nu+2)} \sim \frac{\epsilon^\nu}{\Gamma(\nu+2)} \quad \text{as } \epsilon \rightarrow 0+, \quad (F-5)$$

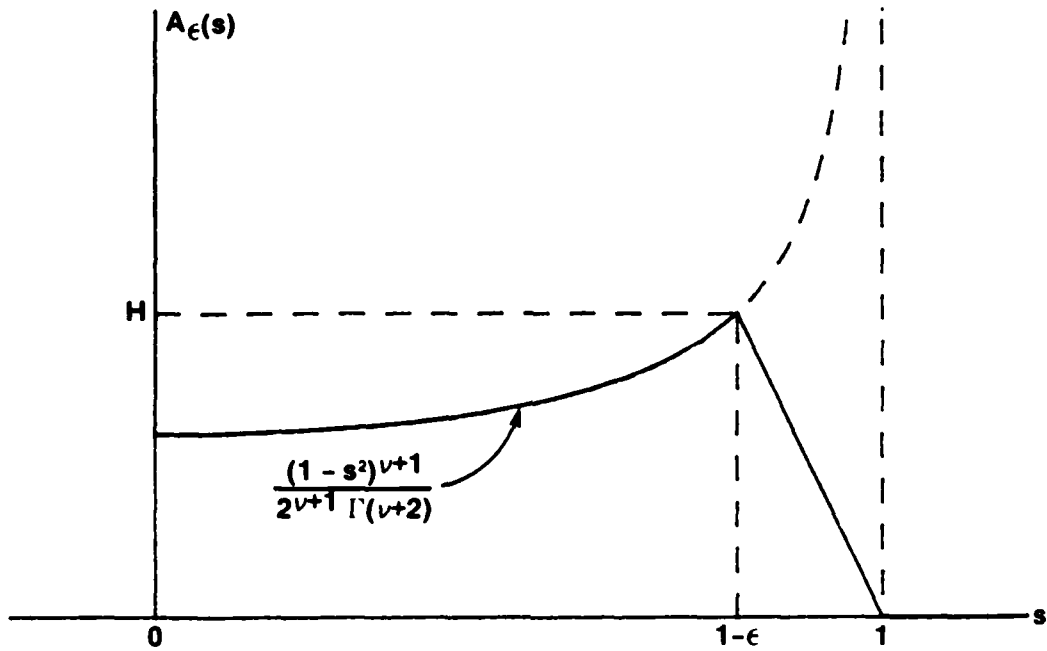


Figure F-1. Approximation to Auxiliary Function $A(s)$

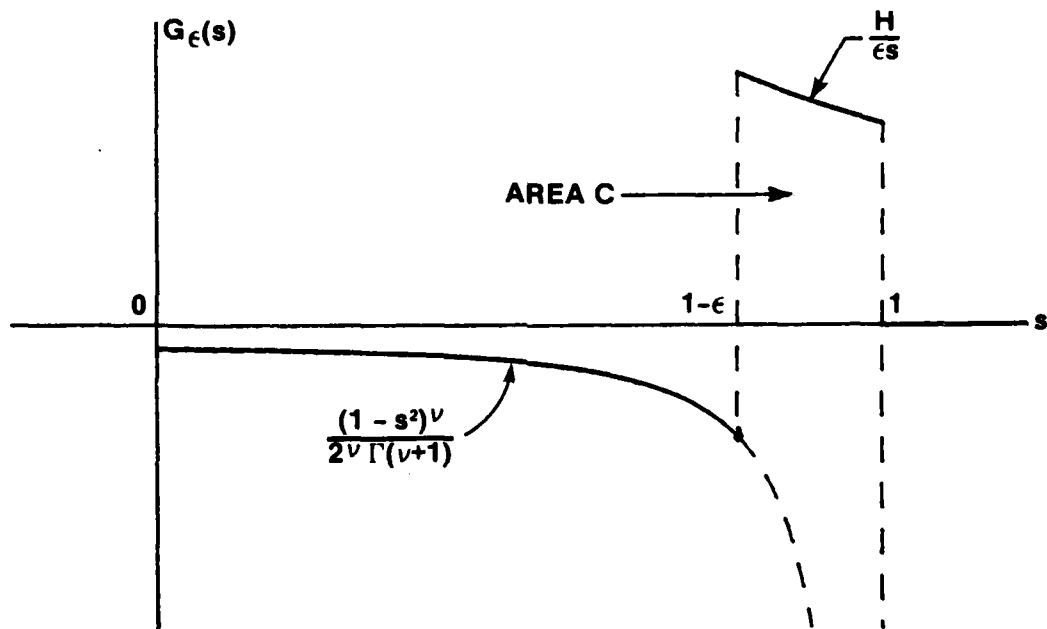


Figure F-2. Approximation to Generalized Function $G(s)$

which is tending to infinity since $-2 < \nu < -1$. The area of this positive pulse is

$$C = \int_{1-\epsilon}^1 ds \frac{H}{\epsilon s} = -\frac{H}{\epsilon} \ln(1-\epsilon) \sim \frac{\epsilon^{\nu+1}}{\Gamma(\nu+2)} \quad \text{as } \epsilon \rightarrow 0+. \quad (\text{F-6})$$

This area is also tending to $+\infty$ as $\epsilon \rightarrow 0+$; recall (F-4). The rate of increase of C is greater, the closer ν is to -2 . (For $\nu \rightarrow -1$, $H \rightarrow 1$, $C \rightarrow \frac{-1}{\epsilon} \ln(1-\epsilon)$; thus area $C \sim 1$ as $\epsilon \rightarrow 0+$. This is the unit area impulse presented in (49) for $\nu = -1$.)

Figure F-2 is one approximation to generalized function $G(s)$ defined in (E-31). Its most important feature is the impulsive-like positive pulse near $s = 1$. An alternative approximation is afforded in figure F-3, where the area \tilde{C} of the impulse at $s = 1$ is given by (recall (F-6))

$$\tilde{C} = \frac{\epsilon^{\nu+1}}{\Gamma(\nu+2)}. \quad (\text{F-7})$$

The notation used in (E-31) for the generalized function,

$$G(s) = \frac{(1-s^2)^\nu}{2^\nu \Gamma(\nu+1)} \Big|_G, \quad (\text{F-8})$$

conceals the positive impulsive behavior at $s = 1$ that the series of approximations in figures F-1 through F-3 indicate must be present. In fact, (F-8) is negative for $0 \leq s < 1$, by reference to (F-4).

The alternative approximation we obtain to weighting (50) is then, from (E-29) and figure F-3,

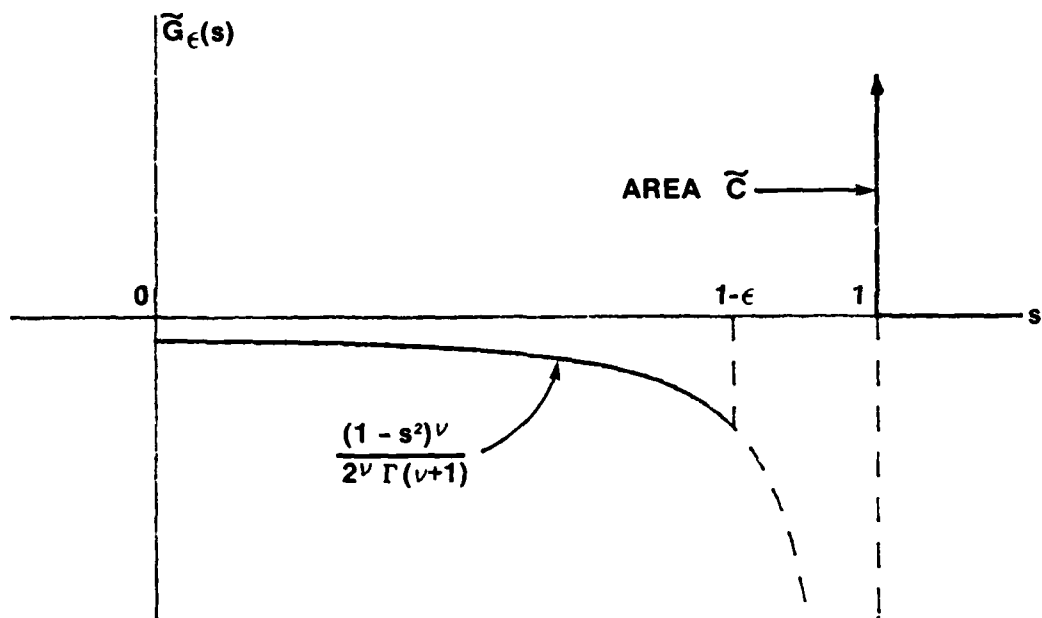


Figure F-3. An Alternative Approximation to Generalized Function $G(s)$

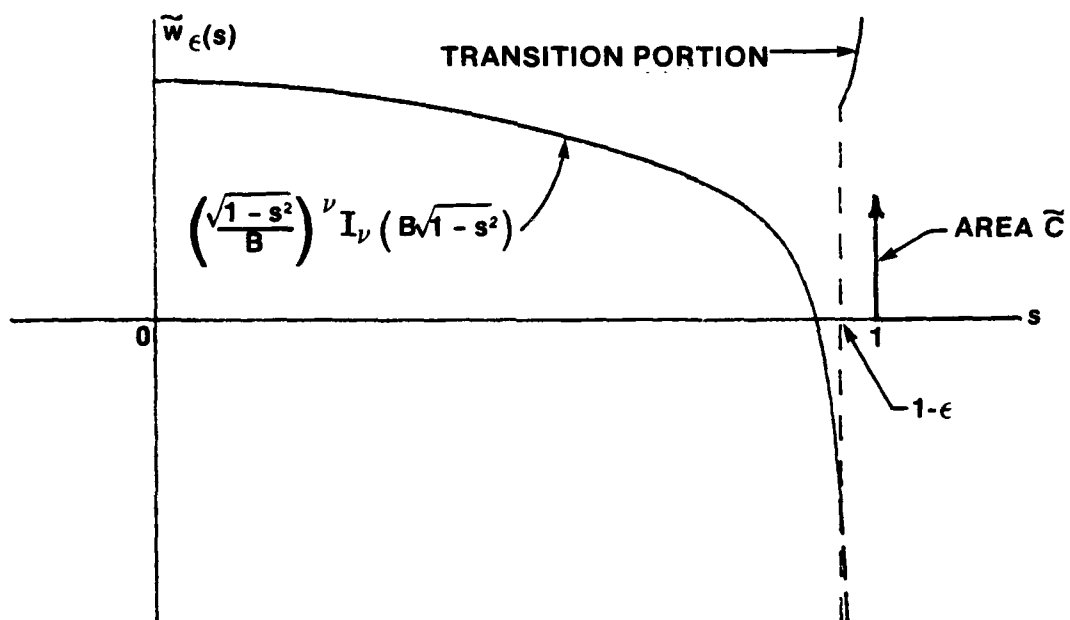


Figure F-4. An Approximation to Weighting (50)

$$\begin{aligned} \tilde{w}_\epsilon(s) &= D(s) + \tilde{G}_\epsilon(s) \\ &= \left\{ \begin{array}{ll} \left(\frac{\sqrt{1-s^2}}{B} \right)^\nu I_\nu(B\sqrt{1-s^2}) & \text{for } 0 < s < 1-\epsilon \\ \left(\frac{\sqrt{1-s^2}}{B} \right)^\nu I_\nu(B\sqrt{1-s^2}) - \frac{(1-s^2)^\nu}{2^\nu \Gamma(\nu+1)} & \text{for } 1-\epsilon < s < 1 \end{array} \right\} + \tilde{C} \delta(s-1). \quad (F-9) \end{aligned}$$

The plot in figure F-4 illustrates this approximation. The "transition portion" in $(1-\epsilon, 1)$, which is the bottom line of (F-9), is singular at $s = 1$; however, this is an integrable singularity, as may be seen by reference to (E-29) and (E-30). The impulse at $s = 1$ is of finite area \tilde{C} given by (F-7).

As $\epsilon \rightarrow 0+$, area \tilde{C} of the impulse tends to infinity; see (F-7) and (F-4). However, the area under the main portion of the approximation $\tilde{w}_\epsilon(s)$ precisely cancels this singular behavior; that is, as $\epsilon \rightarrow 0+$,

$$\begin{aligned} \int_a^{1-\epsilon} ds \left(\frac{\sqrt{1-s^2}}{B} \right)^\nu I_\nu(B\sqrt{1-s^2}) &\sim \int_a^{1-\epsilon} ds \frac{(1-s)^\nu}{\Gamma(\nu+1)} \\ &= \frac{(1-a)^{\nu+1} - \epsilon^{\nu+1}}{\Gamma(\nu+2)} \sim -\frac{\epsilon^{\nu+1}}{\Gamma(\nu+2)}, \quad (F-10) \end{aligned}$$

which is $-\tilde{C}$. Since the area under the transition portion is

$$\int_{1-\epsilon}^1 ds D(s) \sim \int_{1-\epsilon}^1 ds \frac{B^2(1-s)^{\nu+1}}{2^\nu \Gamma(\nu+2)} = \frac{B^2 \epsilon^{\nu+2}}{2^\nu \Gamma(\nu+3)} \quad \text{as } \epsilon \rightarrow 0+, \quad (F-11)$$

which tends to 0 as $\epsilon \rightarrow 0+$, the area under approximation $\tilde{w}_\epsilon(s)$ remains finite as $\epsilon \rightarrow 0+$. Indeed it must remain finite, because Hankel transform (12) or (15) must remain finite in order to realize pattern (48), which is entire in u , v , u , and B .

Thus our final approximation to $w(s)$ is simply

$$\hat{w}_\epsilon(s) = \left\{ \begin{array}{ll} \left(\frac{\sqrt{1-s^2}}{B} \right)^\nu I_\nu \left(B \sqrt{1-s^2} \right) & \text{for } 0 < s < 1-\epsilon \\ 0 & \text{for } 1-\epsilon < s < 1 \end{array} \right\} + \tilde{C} \delta(s-1), \quad (\text{F-12})$$

and is shown in figure F-5. It is very important to observe that the simple expedient of approximating $w(s)$ by

$$\left\{ \begin{array}{ll} \left(\frac{\sqrt{1-s^2}}{B} \right)^\nu I_\nu \left(B \sqrt{1-s^2} \right) & \text{for } 0 < s < 1-\epsilon \\ 0 & \text{otherwise} \end{array} \right\} \quad (\text{F-13})$$

is totally inadequate because, as $\epsilon \rightarrow 0^+$, the area under the cusp at $s = 1-\epsilon$ tends to infinity, and cannot possibly yield an entire function for the pattern. The impulse is necessary to compensate for the singular behavior of (F-13) near $s = 1$; it allows us to realize the "finite part" of the Hankel transform of (F-13) for $\epsilon = 0$.

(As $\nu \rightarrow -1$, the value of \tilde{C} in (F-7) tends to the finite value 1, which is the impulse in (49). And as $\nu \rightarrow -2$, the doublet of (51) could probably be extracted as a limit from (F-12); this procedure has not been pursued.)

The result of using approximation (F-12) with (F-7), for $\nu = -1.5$ and $B = 4$, is displayed as the patterns in figures F-6 through F-8 for $\epsilon = .1, .01, .001$, respectively. We have selected $\mu = 0$, that is, two dimensions, and are approximating the ideal pattern for $B = 4$ shown in figure 13. It is seen that the approximations become progressively better as ϵ decreases, and that the result in figure F-8 is indeed very close to figure 13.

The approximation $\hat{w}_\epsilon(s)$ in (F-12) and figure F-5 used, for the impulse area, the value \tilde{C} given by (F-7) as a limit of (F-6) for small ϵ . A better approach is not to use the limiting value, but to use the actual value of the pertinent function, since we would like good approximations for moderate values of ϵ , not just very small ϵ . This procedure is considered in detail in [12], with the result

$$\begin{aligned} \bar{w}_\epsilon(s) = & \left(\frac{\sqrt{1-s^2}}{B} \right)^\nu I_\nu \left(B \sqrt{1-s^2} \right) U(1-\epsilon-s) \\ & + \left(\frac{\sqrt{2\epsilon-\epsilon^2}}{D} \right)^{\nu+1} I_{\nu+1} \left(B \sqrt{2\epsilon-\epsilon^2} \right) \delta(s-1). \end{aligned} \quad (F-14)$$

The patterns for this approximation are depicted in figures F-9 through F-11. The result in figure F-11 for $\epsilon = .1$ is now better than the result for $\epsilon = .001$ in figure F-8; and all we have done is to modify the area of the impulse at $s = 1$. The result for $\epsilon = .15$ in figure F-10 indicates a modest change from the ideal and would be acceptable in some cases. The program for the pattern evaluation is listed at the end of this appendix.

Another possibility is to relocate the impulse in $(1-\epsilon, 1)$ to best approximate the ideal pattern in figure 13. More generally, a shaped narrow pulse, which is concentrated toward the boundary at $s = 1$, could be used; these possibilities are discussed further in [12].

Some additional results involving delta functions and Bessel transforms are given here in appendix H.

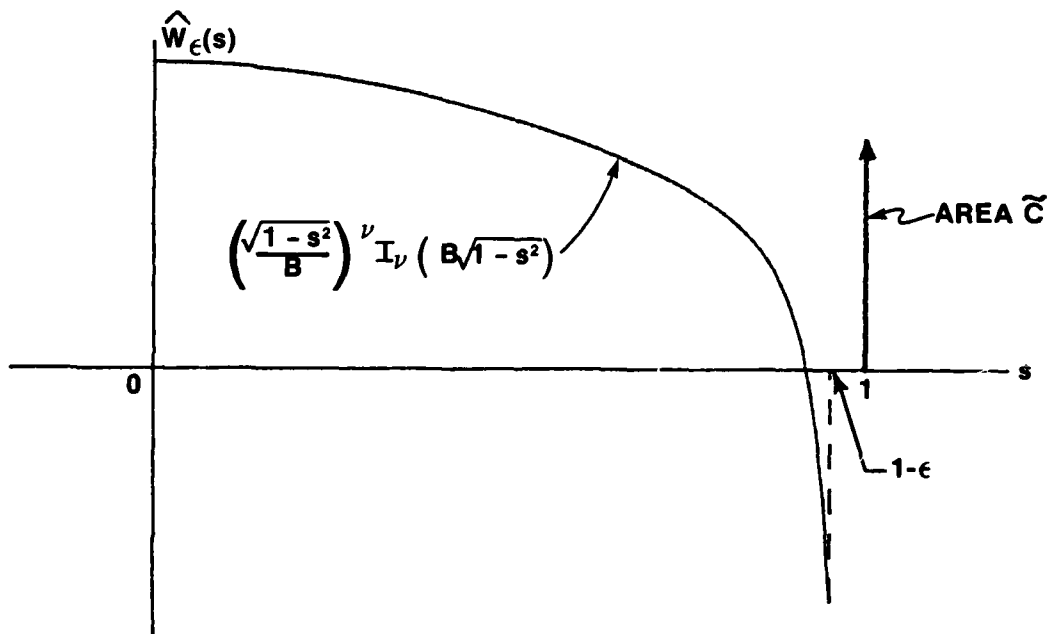


Figure F-5. Final Approximation to Weighting (50)

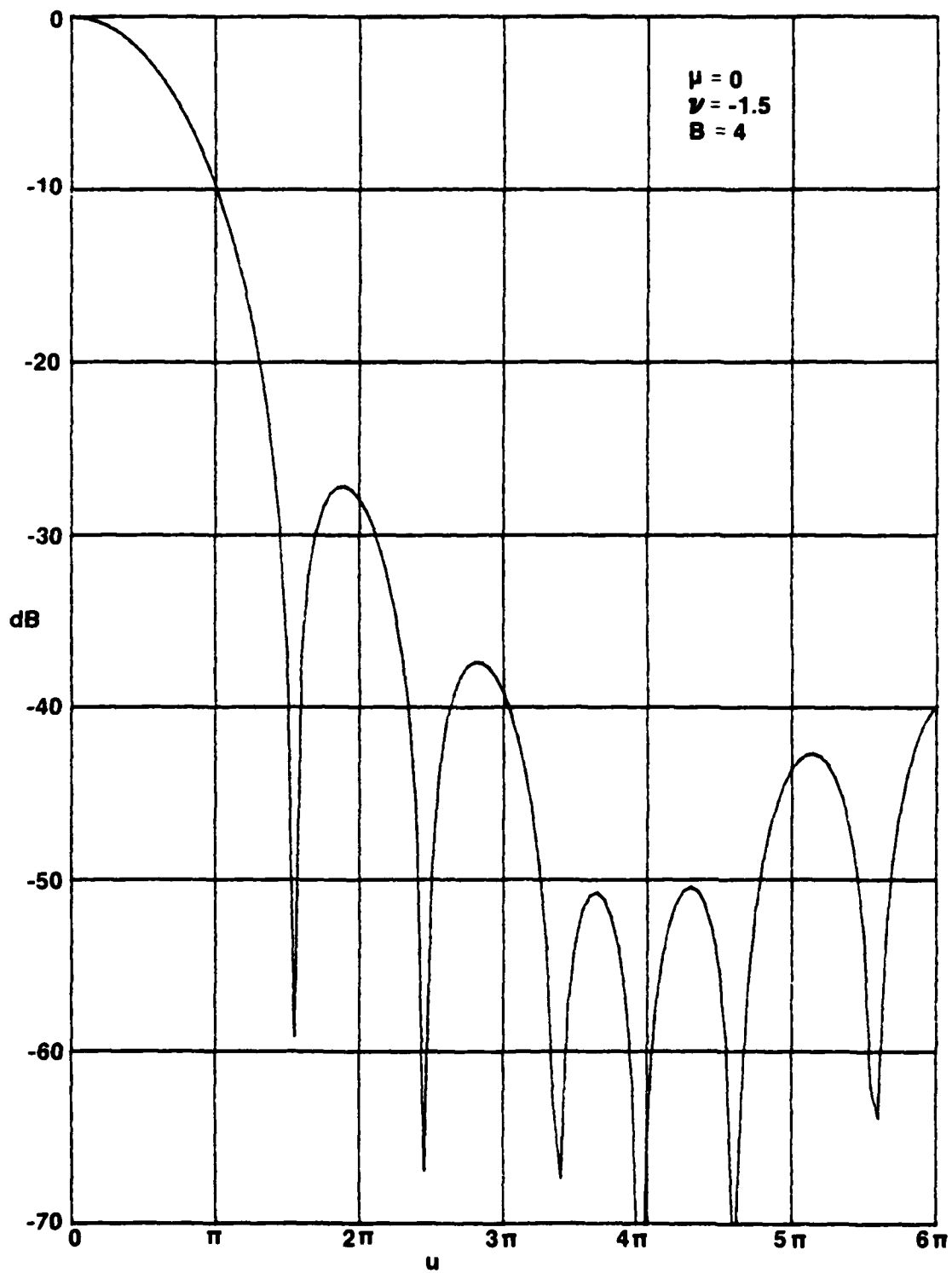


Figure F-6. Pattern of Approximation (F-12) for $\epsilon = .1$

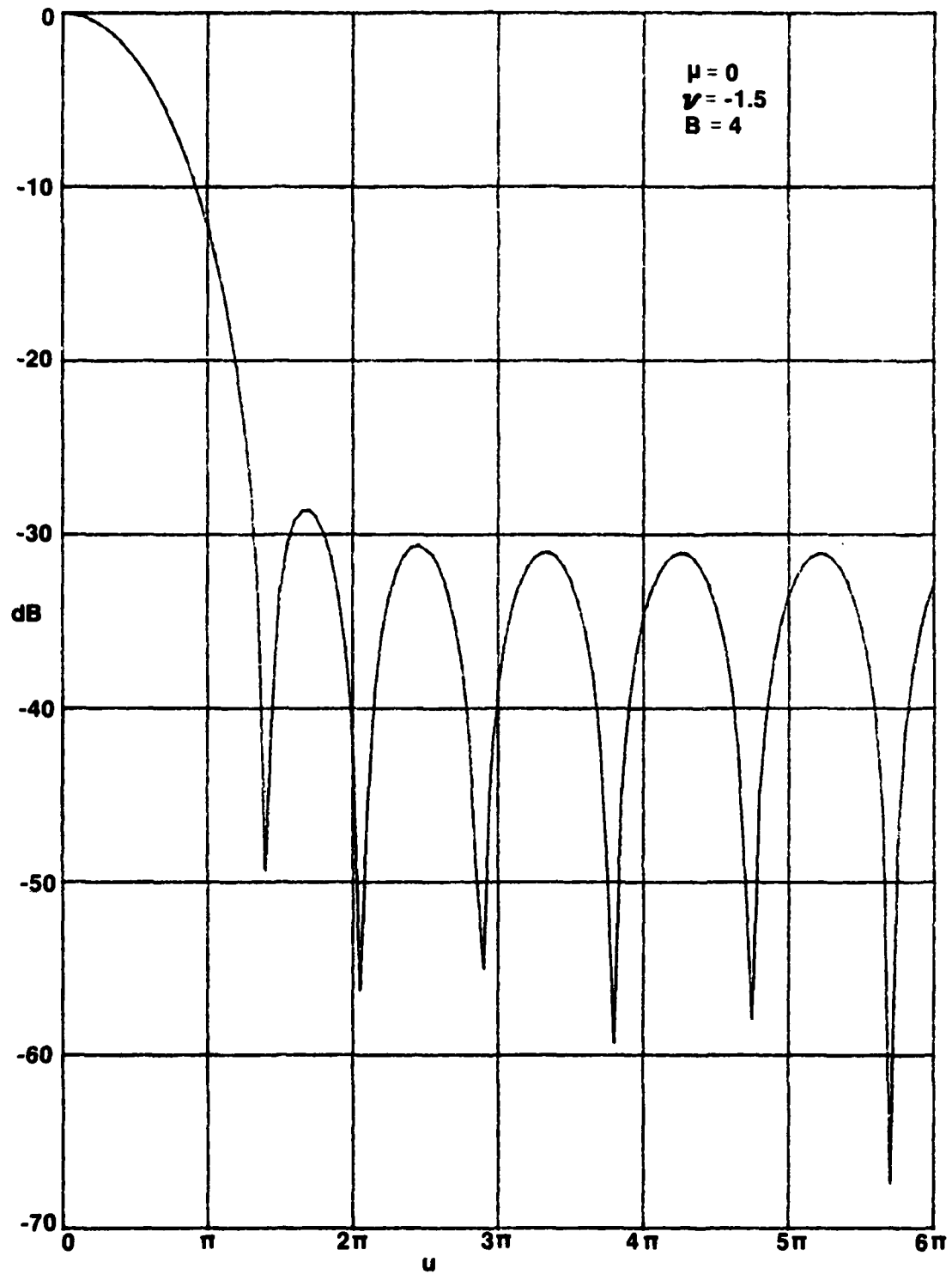


Figure F-7. Pattern of Approximation (F-12) for $\epsilon = .01$

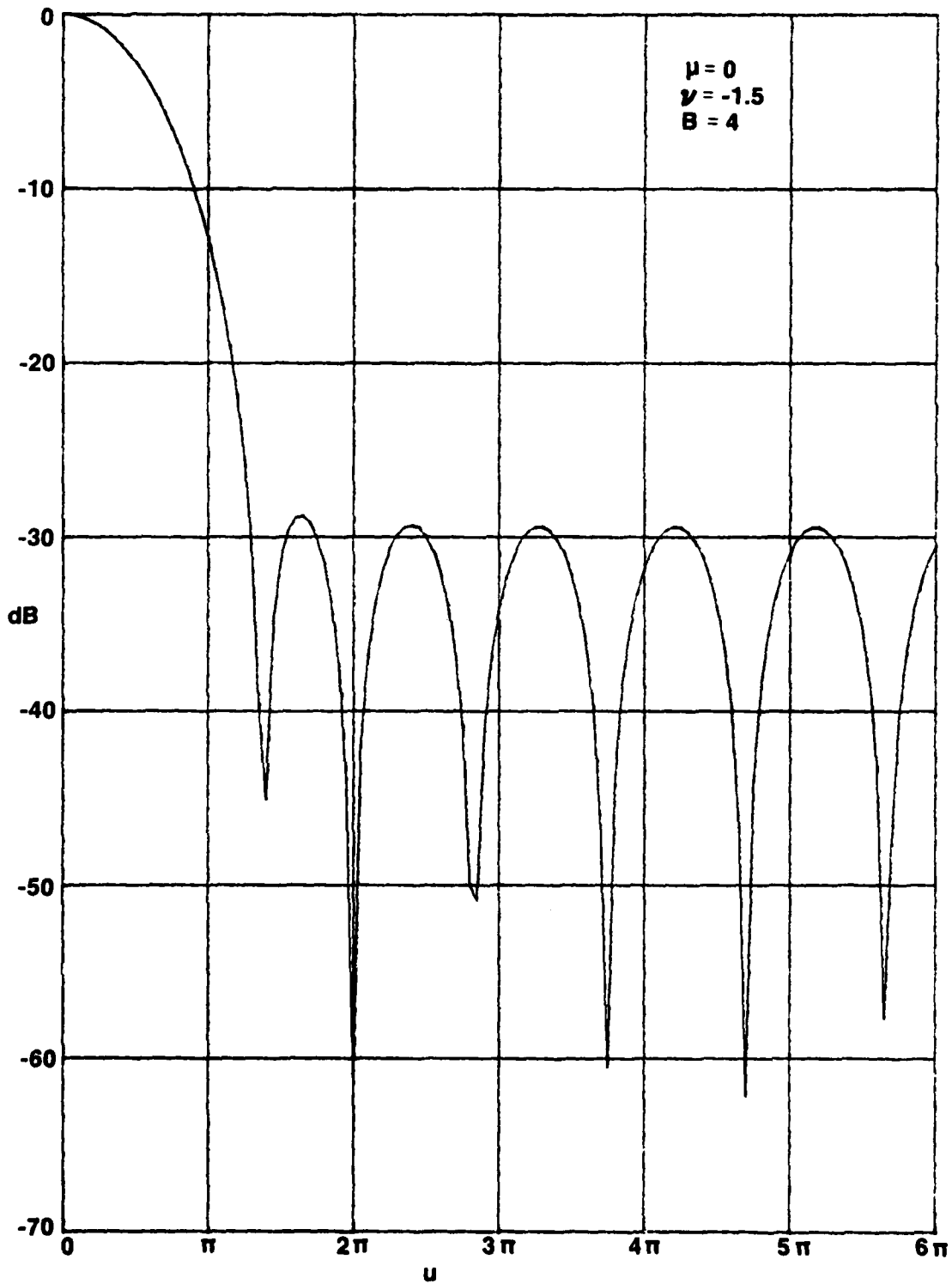


Figure F-8. Pattern of Approximation (F-12) for $\epsilon = .001$

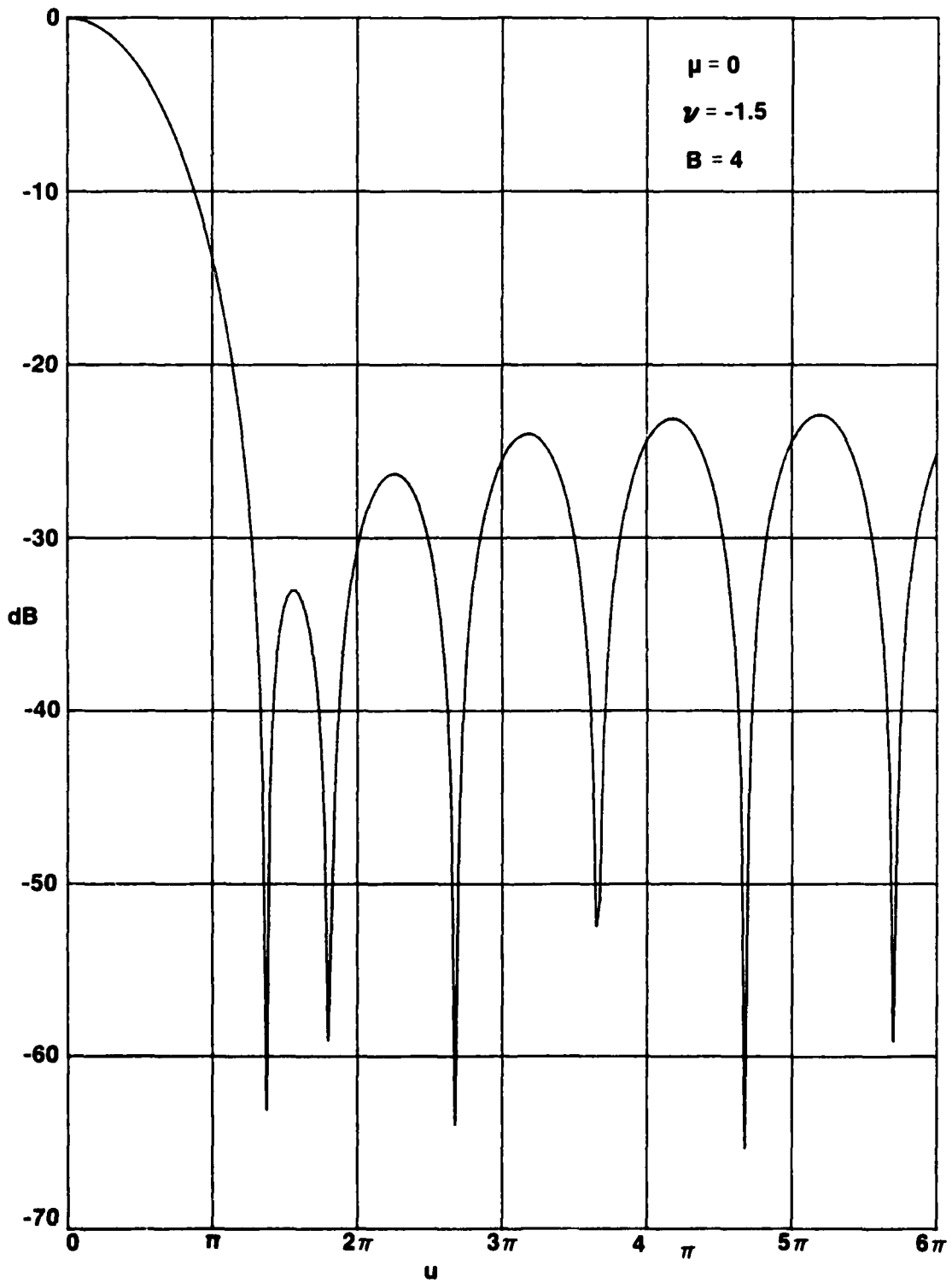


Figure F-9. Pattern of Approximation (F-14) for $\epsilon = .2$

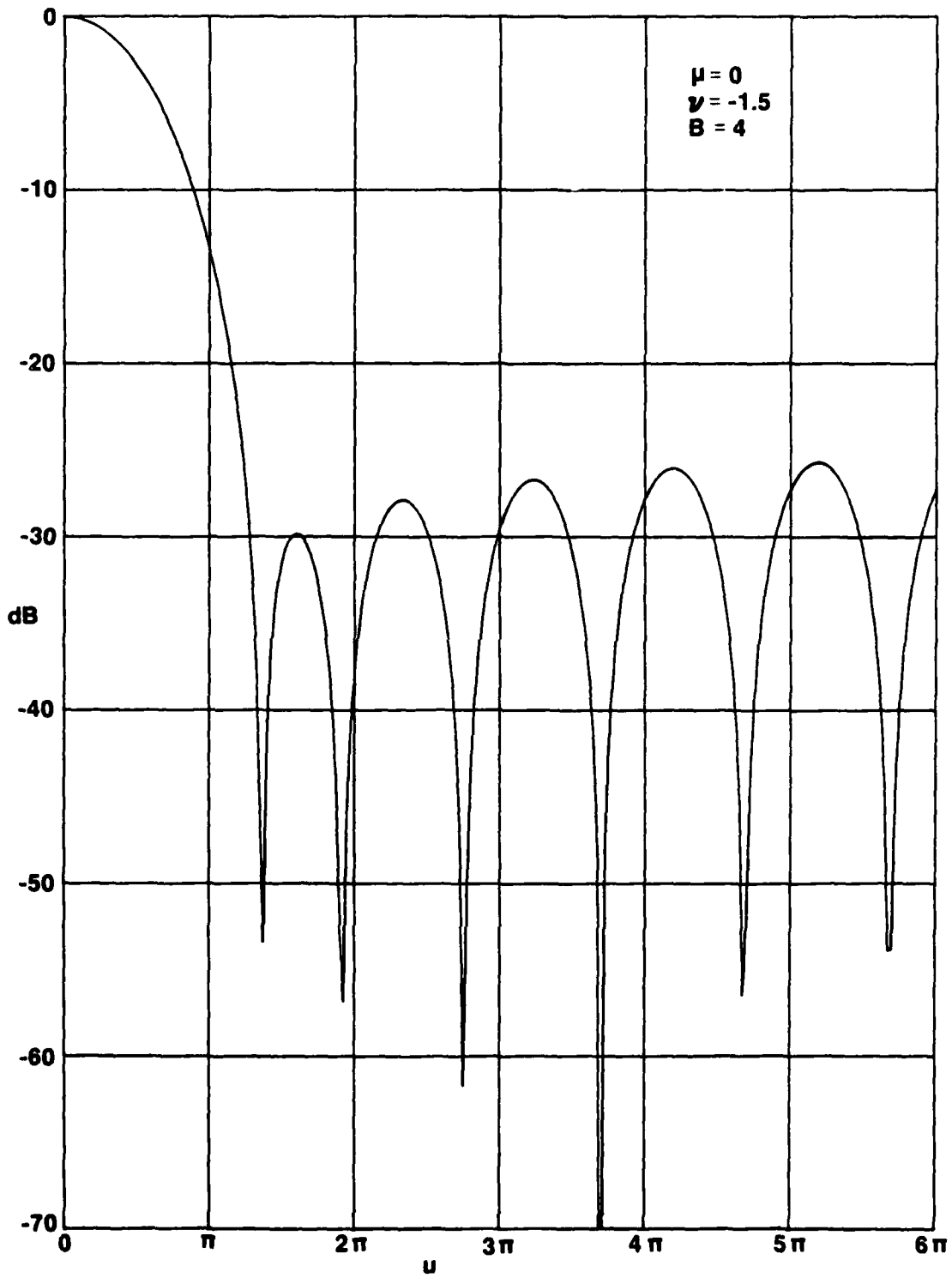
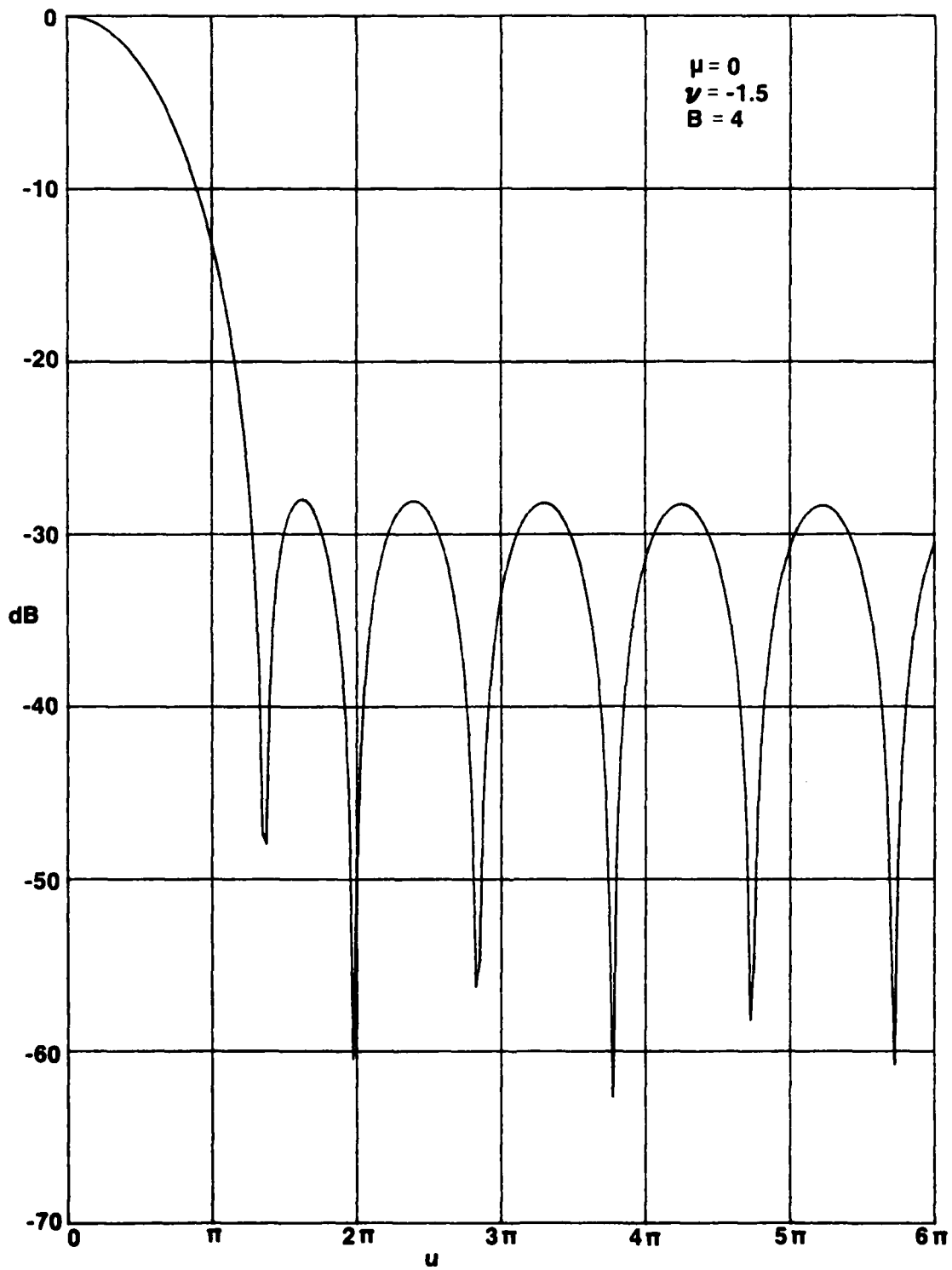


Figure F-10. Pattern of Approximation (F-14) for $\epsilon = .15$

Figure F-11. Pattern of Approximation (F-14) for $\epsilon = .1$

PROGRAM FOR PATTERN EVALUATION

```

10  Eps=.1      ! Pattern for Weighting (F=14)
20  Mu=0
30  Nu=-1.5
40  Bc=4
50  DIM G(0:240)
60  COM U, Bc, Mu, Nu, M21
70  M21=Mu*2+1
80  T=2*Eps-Eps^2
90  F1e=T*(Nu+1)*FNInuxnu(Nu+1, Bc*SQR(T))
100 R=0
110 B=1-Eps
120 FOR Iu=0 TO 240
130 U=Iu*PI/40
140 S=(FNS(A)+FNS(B))*0.5
150 N=2
160 H=(B-A)*0.5
170 F=(B-A)/3
180 Vo=9E99
190 T=0
200 FOR k=1 TO N-1 STEP 2
210 T=T+FNS(R+H*k)
220 NEXT K
230 S=S+T
240 V=(S+T)*F
250 IF ABS(V-Vo)<=ABS(V)*1E-4 THEN 310
260 Vo=V
270 N=N*2
280 H=H*.5
290 F=F*.5
300 GOTO 190
310 G(Iu)=F1e*FNJnuxnu(Mu, U)+V      ! Voltage Response
320 PRINT Iu, G(Iu)
330 NEXT Iu
340 PLOTTER IS "9872A"
350 LIMIT 25, 175, 35, 245
360 OUTPUT 705; "VS5"
370 SCALE 0, 240, -70, 0
380 GRID 40, 10
390 PENUP
400 FOR Iu=0 TO 240
410 PLOT Iu, 20*LGT(ABS(G(Iu)/G(0)))
420 NEXT Iu
430 PENUP
440 END
450 !
460 DEF FNS(S)
470 COM U, Bc, Mu, Nu, M21
480 T=1-S*S
490 T1=FNJnuxnu(Mu, U+S)
500 T2=FNInuxnu(Nu, Bc*SQR(T))
510 RETURN S^M21*T^Nu*T1*T2
520 FNEND
530 !

```

FNJnuxnu and FNInuxnu are listed in Appendix D

Appendix G
EVALUATION OF A BESSEL INTEGRAL VIA RECURSION

The integral of interest is

$$g_\nu(u, B) \equiv \int_0^1 ds K(u, s) \left(\frac{B}{\sqrt{1-s^2}} \right)^\nu I_\nu \left(B \sqrt{1-s^2} \right), \quad (G-1)$$

where the kernel K is the Bessel function as given in (11). We have, via [5; 9.6.28],

$$\begin{aligned} \frac{\partial}{\partial B} g_\nu(u, B) &= \int_0^1 ds K(u, s) B \left(\frac{B}{\sqrt{1-s^2}} \right)^{\nu-1} I_{\nu-1} \left(B \sqrt{1-s^2} \right) \\ &= B g_{\nu-1}(u, B). \end{aligned} \quad (G-2)$$

(This relation actually holds for any kernel K , not just (11).) Since, from (G-1),

$$g_\nu(u, 0) = 0 \quad \text{if } \nu > 0,$$

we have the integral recursion

$$g_\nu(u, B) = \int_0^B dt t g_{\nu-1}(u, t) \quad \text{for } \nu > 0. \quad (G-3)$$

We already know the starting case of

$$g_0(u, B) = \int_0^1 ds s \left(\frac{s}{u} \right)^\mu J_\mu(us) I_0 \left(B \sqrt{1-s^2} \right) = J_{\mu+1} \left(\sqrt{u^2 - B^2} \right); \quad (G-4)$$

see (23). Substitution in (G-3) yields

$$\begin{aligned}
 g_1(u, B) &= \int_0^B dt \, t \, J_{u+1}(\sqrt{u^2 - t^2}) = \int_{\sqrt{u^2 - B^2}}^u dx \, x \, J_{u+1}(x) \\
 &= J_u(\sqrt{u^2 - B^2}) - J_u(u),
 \end{aligned} \tag{G-5}$$

where we employed (21).

Now we employ (G-3) and (G-5):

$$\begin{aligned}
 g_2(u, B) &= \int_0^B dt \, t \left[J_u(\sqrt{u^2 - t^2}) - J_u(u) \right] \\
 &= J_{u-1}(\sqrt{u^2 - B^2}) - J_{u-1}(u) - \frac{B^2}{2} J_u(u);
 \end{aligned} \tag{G-6}$$

the integral evaluation follows from direct comparison with (G-5).

The last case for $\nu = 3$ follows in similar fashion:

$$g_3(u, B) = J_{u-2}(\sqrt{u^2 - B^2}) - J_{u-2}(u) - \frac{1}{2} B^2 J_{u-1}(u) - \frac{1}{8} B^4 J_u(u). \tag{G-7}$$

Appendix H
TWO BESSEL INTEGRALS THAT YIELD GENERALIZED FUNCTIONS

The starting point is the Hankel transform pair in (15) and (16). If we let $w(s) = \delta(s-a)$ (where $a > 0$) in (15), we get

$$g(u) = a \left(\frac{a}{u}\right)^\mu J_\mu(au) \quad \text{for } u > 0. \quad (\text{H-1})$$

Substituting (H-1) in (16) then yields the useful relation

$$\int_0^\infty du u J_\mu(su) J_\mu(au) = \frac{1}{a} \delta(s-a). \quad (\text{H-2})$$

On the other hand, if we let the weighting be a doublet,

$$w(s) = \frac{1}{s} \delta'(s-a), \quad \text{then } g(u) = -u \left(\frac{a}{u}\right)^\mu J_{\mu-1}(au). \quad (\text{H-3})$$

The inverse relation (16) yields

$$-\left(\frac{s}{a}\right)^\mu \frac{1}{s} \delta'(s-a) = \int_0^\infty du u^2 J_\mu(su) J_{\mu-1}(au). \quad (\text{H-4})$$

However, since

$$\begin{aligned} f(s) \delta'(s-a) &= [f(a) + f'(a)(s-a) + \dots] \delta'(s-a) \\ &= f(a) \delta'(s-a) - f'(a) \delta(s-a), \end{aligned} \quad (\text{H-5})$$

then

$$\int_0^\infty du u^2 J_\mu(su) J_{\mu-1}(au) = -\frac{1}{a} \delta'(s-a) + \frac{\mu-1}{a^2} \delta(s-a). \quad (\text{H-6})$$

Equations (H-2) and (H-6) are the desired results.

REFERENCES

1. F. J. Harris, "On the Use of Windows for Harmonic Analysis with the Discrete Fourier Transform," Proc. IEEE, vol. 66, no. 1, January 1978, pp. 51-83.
2. A. H. Nuttall, "Some Windows with Very Good Sidelobe Behavior," IEEE Trans. on Acoustics, Speech, and Signal Processing, vol. ASSP-29, no. 1, February 1981, pp. 84-91; also NUSC Technical Report 6239, 9 April 1980.
3. J. F. Kaiser, "Digital Filters" in System Analysis by Digital Computer, F. F. Kuo and J. F. Kaiser, editors, J. Wiley and Sons, NY, 1966, pp. 218-285.
4. J. F. Kaiser and R. W. Schafer, "On the Use of the I_0 -Sinh Window for Spectrum Analysis," IEEE Trans. on Acoustics, Speech, and Signal Processing, vol. ASSP-28, no. 1, February 1980, pp. 105-107.
5. Handbook of Mathematical Functions, U. S. Dept. of Commerce, National Bureau of Standards, Applied Math. Series 55, U.S. Govt. Printing Office, June 1964.
6. W. Magnus and F. Oberhettinger, Formulas and Theorems for the Functions of Mathematical Physics, Chelsea Publishing Co., N.Y., 1954.
7. G. N. Watson, Theory of Bessel Functions, Cambridge University Press, London, England, Second Edition, 1958.
8. R. L. Streit, "A Two-Parameter Family of Weights for Nonrecursive Digital Filters and Antennas," submitted to IEEE Trans. on Antennas, 21 April 1982.
9. G. J. van der Maas, "A Simplified Calculation for Dolph-Chebyshev Arrays," Journal of Applied Physics, vol. 25, no. 1, January 1954, pp. 121-124.
10. I. S. Gradshteyn and I. M. Ryzhik, Table of Integrals, Series, and Products, Academic Press, Inc., N.Y., 1980.

TR 6761

11. A. H. Nuttall, Probability Distribution of Array Response for Randomly Perturbed Element Gains, NUSC Technical Report 5687, 29 September 1977.
12. A. H. Nuttall, Approximations to Some Generalized Functions; Application to Array Processing, NUSC Technical Report 6767, 19 July 1982

INITIAL DISTRIBUTION LIST

Addressee	No. of Copies
ASN (RE&S)	1
OUSDR&E (Research & Advanced Technology)	2
Deputy USDR&E (Res & Adv Tech)	1
OASN, Dep Assist Secretary (Res & Adv Tech)	1
ONR, ONR-100, -102, -200, -400, -410, -422, -425, -425AC, -430,	9
CNO, OP-090, -098, -902, -941, -951, -951D, -951E, -952, -96,	
-981F, -981, -982F, -983	13
CNM, MAT-00, -05, SP-20, -24, ASW-12, -11, -13, -14, MAT-03621,	
Systems Project Office (PM-2) Trident,	
Surface Ships Project Office (PM-18)	11
DIA, DT-2C	1
NRL	1
NRL, USRD	1
NRL, AESD	1
NORDA	1
USOC, Code 241, 240	2
SUBBASE LANT	1
OCEANAV	1
NEOC	1
NWOC	1
NAVOCEANO, Code 02, 3400, 6200	3
NAVELECSYSCOM, ELEX 00, 03, 320	3
NAVSEASYSYSCOM, Sea-00, -003, -03R, -05R, -611, -613, -62R, -63R,	
-63R-1, -631Y, -631Y (Surface Sys Sub-Gr), SEA-92R,	12
NAVAIRDEVCEN	1
NAVAIRDEVCEN, Key West	1
NOSC	1
NOSC, Code 6565 (Library)	1
NAVWPNSCEN	1
NCSC	1
CIVENGRLAB	1
NAVSURFWPNCEN	1
NAV SURFACE WEAPONS CENTER, WHITE OAK LAB	1
NAVTRAEQUIPCENT Technical Library	1
NAVPGSCOL	1
NAVAIRTESTCEN	1
APL/UW, SEATTLE	1
ARL/PENN STATE, STATE COLLEGE	1
CENTER FOR NAVAL ANALYSES (ACQUISITION UNIT)	1
DTIC	1
DARPA	1
NOAA/ERL	1
NATIONAL RESEARCH COUNCIL	1
WEAPON SYSTEM EVALUATION GROUP	1
WOODS HOLE OCEANOGRAPHIC INSTITUTION	1
ENGINEERING SOCIETIES LIB, UNITED ENGRG CTR	1
ARL, UNIV OF TEXAS	1
MARINE PHYSICAL LAB, SCRIPPS	1

INITIAL DISTRIBUTION LIST (CONT'D)

Addressee	No. of Copies
INTERMETRICS INC. EAST LYME, CT	1
MAR, INC. EAST LYME, CT	1
EG&G WASHINGTON ANAL SER CTR, INC. (T. Russell)	1
HYDROTRONICS INC. (D. Clark)	1
ANALYSIS & TECHNOLOGY, INC., N. STONINGTON (T. Dziedzic)	1
EDO CORPORATION, NY (J. Vincenzo)	1
Dr. David Middleton, 127 East 91st Street, New York, NY 10028	1
Prof. Louis Scharf, Dept. of Electrical Engin., University of Rhode Island, Kingston, RI 02881	1
Prof. Donald Tufts, Dept. of Electrical Engin., University of Rhode Island, Kingston, RI 02881	1
S. L. Marple, The Analytic Sciences Corp., 8301 Greensboro Drive, McLean, VA 22102	1
T. E. Barnard, Chesapeake Instrument Div., Gould Inc., Glen Burnie, Md 21061	1
Prof. P. M. Schultheiss, Dept. of Electrical Engin., P.O. Box 2157, Yale University, 15 Prospect Street, New Haven, CT 06520	1
Dr. Allan G. Piersol, Bolt, Beranek, and Newman, 21120 Van Owen St., P.O. Box 633, Canoga Park, CA 92305	1
Prof. Y. T. Chan, Dept. of Electrical Engin., Royal Military College, Kingston, Ontario, Canada K7L 2W3	1